EJN European Journal of Neuroscience

FENS Federation of European Neuroscience Societies

European Journal of Neuroscience, Vol. 41, pp. 1553–1568, 2015 doi:10.1111/ejn.12905

BEHAVIORAL NEUROSCIENCE

Genetic mapping of ASIC4 and contrasting phenotype to ASIC1a in modulating innate fear and anxiety

Shing-Hong Lin,[1,2] Ya-Chih Chien,[2] Wei-Wei Chiang,[3] Yan-Zhen Liu,[3] Cheng-Chang Lien[4] and Chih-Cheng Chen[1,2,3]

[1]Graduate institute of Life Sciences, National Defense Medical Center, Taipei, Taiwan
[2]Institute of Biomedical Sciences, Academia Sinica, Taipei 115, Taiwan
[3]Taiwan Mouse Clinic-National Comprehensive Mouse Phenotyping and Drug Testing Center, Academia Sinica, Taipei, Taiwan
[4]Institute of Neuroscience, National Yang-Ming University, Taipei, Taiwan

Keywords: ASIC, behavioral phenotyping, Cre, interneuron, knockout mice

Abstract

Although ASIC4 is a member of the acid-sensing ion channel (ASIC) family, we have limited knowledge of its expression and physiological function *in vivo*. To trace the expression of this ion channel, we generated the ASIC4-knockout/CreERT^2-knockin (*Asic4*^{CreERT2}) mouse line. After tamoxifen induction in the *Asic4*^{CreERT2}::CAG-STOP^{floxed}-Td-tomato double transgenic mice, we mapped the expression of ASIC4 at the cellular level in the central nervous system (CNS). ASIC4 was expressed in many brain regions, including the olfactory bulb, cerebral cortex, striatum, hippocampus, amygdala, thalamus, hypothalamus, brain stem, cerebellum, spinal cord and pituitary gland. Colocalisation studies further revealed that ASIC4 was expressed mainly in three types of cells in the CNS: (i) calretinin (CR)-positive and/or vasoactive intestine peptide (VIP)-positive interneurons; (ii) neural/glial antigen 2 (NG2)-positive glia, also known as oligodendrocyte precursor cells; and (iii) cerebellar granule cells. To probe the possible role of ASIC4, we hypothesised that ASIC4 could modulate the membrane expression of ASIC1a and thus ASIC1a signaling *in vivo*. We conducted behavioral phenotyping of *Asic4*^{CreERT2} mice by screening many of the known behavioral phenotypes found in *Asic1a* knockouts and found ASIC4 not involved in shock-evoked fear learning and memory, seizure termination or psychostimulant-induced locomotion/rewarding effects. In contrast, ASIC4 might play an important role in modulating the innate fear response to predator odor and anxious state because ASIC4-mutant mice showed increased freezing response to 2,4,5-trimethylthiazoline and elevated anxiety-like behavior in both the open-field and elevated-plus maze. ASIC4 may modulate fear and anxiety by counteracting ASIC1a activity in the brain.

Introduction

In mammals, the acid-sensing ion channel (ASIC) family contains four genes (*Accn1–4*), which encode six members of ASIC subtypes, including ASIC1a, ASIC1b, ASIC2a, ASIC2b, ASIC3 and ASIC4 (Lin *et al.*, 2015). ASICs are voltage-independent proton-gated ion channels involved in neuron excitability, synaptic modulation, nociception, cardiovascular homeostasis and mechanotransduction (Wu *et al.*, 2012; Chen & Wong, 2013; Omerbašić *et al.*, 2014; Abboud & Benson, 2015; Baron & Lingueglia, 2015; Holzer, 2015; Huang *et al.*, 2015; Krishtal, 2015; Sluka & Gregory, 2015).

First cloned in the human brain and the rat dorsal root ganglia (DRG), ASIC4 is expressed throughout the nervous system and most abundantly in the pituitary gland (Akopian *et al.*, 2000; Grunder *et al.*, 2000). However, the cell types that express ASIC4 are unknown. Like other ASIC subtypes, ASIC4 shares a common structure characterised by two transmembrane domains, a large extracellular loop and intracellular N- and C-terminal domains (Donier *et al.*, 2008; Sherwood *et al.*, 2012). To form a functional ion channel, three subunits of a given ASIC subtype are required to form a homotrimeric or heterotrimeric complex (Jasti *et al.*, 2007; Bartoi *et al.*, 2014). However, heterologous expression studies indicated that ASIC4 is either inactive on its own or the natural ligand for ASIC4 is not a proton, because it cannot form a proton-gated ion channel complex by itself (Akopian *et al.*, 2000; Donier *et al.*, 2008). Donier *et al.* (2008) suggested a potential function of ASIC4 in modulating ASIC1a (and ASIC3), because co-expression of ASIC4 and ASIC1a can reduce the membrane expression and acid-induced inward current of ASIC1a in Chinese hamster ovary cells (Donier *et al.*, 2008). Therefore, at least at the molecular level, ASIC4 might have a modulatory role when co-expressed with other ASIC subtypes (e.g., ASIC1a). Whether this postulation is true requires mapping evidence to demonstrate that ASIC4 colocalises with the known ASIC subtypes *in vivo*.

In this study, we describe the generation of an *Asic4*-knockout (KO) (*Asic4*$^{-/-}$) mouse line by replacing the CreERT^2 coding sequences with the exon1 (ATG-knockin) of the *Accn4* gene (*Asic4*^{CreERT2}). Subsequent mapping studies with inducible CreERT^2 induction in Cre reporter mice revealed the expression of ASIC4 in

Correspondence: Chih-Cheng Chen, [2]Institute of Biomedical Sciences, as above.
E-mail: chih@ibms.sinica.edu.tw

Received 17 February 2015, revised 25 March 2015, accepted 27 March 2015

the developing nervous system at the single-cell level. In contrast to the broad expression of ASIC1a, ASIC4 is expressed in some limited cell populations in the nervous system. In parallel to this limited expression pattern of ASIC4, behavioral phenotyping of *Asic4*$^{-/-}$ (*Asic4*^{CreERT2}) mice indicated that ASIC4 is involved in only some known phenotypes of *Asic1a*-KO (*Asic1a*$^{-/-}$) mice.

Materials and methods

Animal use and care

Male protamine-Cre transgenic mice (Jackson Lab, Bar Harbor, ME, USA; Stock no. 003328) were used to excise the floxed-pGK-neo cassette in the first generation of *Asic4*$^{-/-}$ (*Asic4*$^{CreERT2/CreERT2}$) mice (Fig. 1). For mapping studies, ROSA26R-lacZ mice (Jackson Lab; Stock no. 003309) and CAG-Td-tomato Cre reporter mice (Jackson Lab; Stock no. 007908) were crossed with *Asic4*^{CreERT2} transgenic mice. *Asic1a*$^{-/-}$ mice were obtained by crossing *Asic1a* conditional KO (*Asic1a*$^{f/f}$) mice (Wu *et al.*, 2013) with protamine-Cre mice. The *Asic1a*$^{-/-}$ and *Asic4*$^{-/-}$ mice used in behavioral studies (unless specifically mentioned) were in a congenic C57BL/6J background; that is, heterozygote *Asic4*$^{+/-}$ and *Asic1a*$^{+/-}$ mice had been backcrossed to pure C57BL/6J mice for at least 10 generations. Male mice at 18–24 weeks were recruited for behavioral tests from different litters of heterozygote inter-breeding. For the study of kainic acid-induced seizure, F5–6 male *Asic4*$^{+/+}$ and *Asic4*$^{-/-}$ littermates derived from

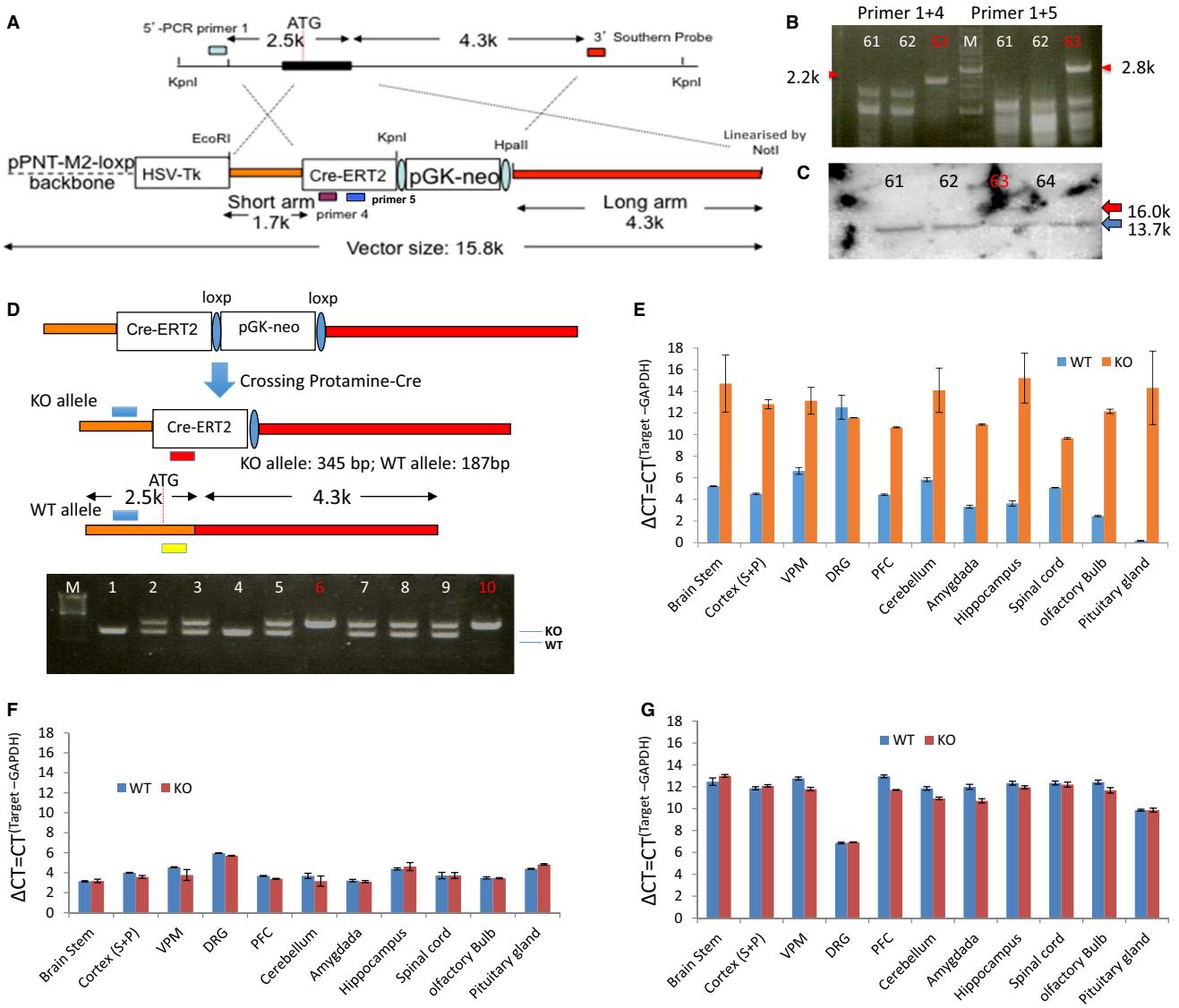

FIG. 1. Generation of ASIC4-KO/CreERT^2-knockin mice. (A) Targeting vector used for ES cell electroporation. After homologous recombination, an ~ 800-bp DNA fragment, corresponding to 267 amino acid peptides in the N-terminus of ASIC4, was deleted. (B) Long-range PCR demonstrated correct homologous recombination of ES cell clone no. 63 with 5′-arm flanking primers used as positions indicated in A. (C) Southern blot of ES cell genomic DNA after KpnI digestion revealed correct homologous recombination of clone no. 63 with a 3′-arm flanking probe used as its location indicated in A. (D) After germline transmission, the positive selection gene floxed-pGK-neo cassette was deleted by crossing the ASIC4-KO mouse with the protamine-Cre transgenic line. Subsequent mice genotyping involved PCR with three primers indicated in the diagram. One litter of heterozygote interbreeding showed that the ASIC4-KO allele was transmitted in a Mendelian ratio. (E) Real-time RT-PCR assay used to confirm the elimination of ASIC4 transcripts in various brain regions from the KO. Target mRNA cycle threshold (CT) value was normalised with the housekeeping gene mouse-GAPDH to obtain the ΔCT value for comparison (n = 3 for each data point). (F) Real-time RT-PCR assay of ASIC1a mRNA expression with KO of ASIC4 in all brain regions and peripheral DRG, and (G) ASIC3 mRNA expression in different tissues from wildtype and ASIC4-KO (n = 3).

Asic4$^{+/-}$ breeding were used. After F11–12 generations, stable *Asic4*$^{-/-}$ and *Asic1a*$^{-/-}$ homozygote colonies were maintained and used in the amphetamine-induced conditioned place preference (CPP) test. For behavioral tests, mice were acclimated to the behavior rearing room for at least 1 week and transported to the behavior testing room at least 1 h before tests. We did our best to minimise the number of animals used, by which only 6–10 mice were used in a behavioral group. All procedures with mice followed the Guide for the Use of Laboratory Animals (US National Research Council, Washington, DC, USA) and were approved by the Institutional Animal Care and Use Committee of Academia Sinica.

Generation and genotyping of Asic4$^{-/-}$ *mice*

The genomic clone (129/Svj) 7k containing Exon1 of *Accn4* was used to generate *Asic4*$^{-/-}$ mice. A 15.8-kb targeting vector was constructed with the CreERT^2 gene (Feil *et al.*, 1997) knocked in to the initiator methionine of ASIC4. A pGK-neo selection cassette flanked by loxP sites was placed downstream of the polyadenylation signal of CreERT^2. A 5′-arm of homology (1.7 kb) and a 3′-arm of homology (4.3 kb) followed by an HSV-TK cassette were placed upstream and downstream of the other components, respectively. Targeting of embryonic stem (ES) cells (129/Sv, R1) and blastocyst microinjection were performed in the Transgenic Core Facility of Academia Sinica. After two trials of ES-cell electroporation, a total of 346 ES clones were obtained and screened for intact homologous recombination by long-range, short-arm flanking PCR and Southern blot analysis. One ES cell clone, no. 63, showing correct homologous recombination in the short arm on PCR and subsequent long arm on Southern blot analysis was chosen for blastocyst microinjection. Chimeras were crossed to wildtype (WT) C57/BL6 mice to generate F1 mice. Founder animals were screened by PCR. For the WT allele (predicted size, 187 bp), we used primers binding to the 5′-UTR (forward primer: 5′-CCTGGTTGCCCTGAGTTTAG-3′) and intron1 (reverse primer: 5′-TTCTCCTTGGGTTTTGCATC-3′). For the knockout (KO) allele (predicted size, 345 bp), we used the WT forward primer combined with the primer targeting the open reading frame of CreERT^2 (reverse primer: 5′-AATCGCGAACATCTTCAGGT-3′).

Real-time RT-PCR

Various central nervous system (CNS) regions and DRG were dissected from ASIC4-KO and their WT siblings. We extracted RNA with TRIzol reagent and performed reverse transcription (RT) with dT18 and Superscript III (Invitrogen) using 2 μg total RNA. RT products were processed with the target primer set and 2 × SYBG premix PCR reagent (Roche, Mannheim, Germany) with the ABI-7300 Real-time PCR system. Expression of target mRNA (target CT) was normalised to the CT value of the housekeeping gene, mouse GAPDH. Delta CT value is defined as $CT^{Target} - CT^{GAPDH}$. The intron-spanning primer sequence used for ASIC1a was forward, 5′-GGCTTCCAGACGTTTGTGTC-3′ and reverse, 5′-TGGTAACAGCATTGCAGGTG-3′; ASIC3, forward, 5′-CCCTGTGGACCTGAGAACTT-3′ and reverse, 5′-CCCTTAGGAGTGGTGAGCAG-3′; ASIC4, forward, 5′-CCATCTGCCCACCAAATATC-3′ and reverse, 5′-GTGTAGGGCAGAAGCATGG-3′; and GAPDH forward, 5′-GGAGCCAAACGGGTCATCATCTC-3′ and reverse, 5′-GAGGGGCCATCCACAGTCTTCT-3′.

Tamoxifen induction in prenatal and adult mice

To map the expression of ASIC4, two lines of Cre reporter mice, ROSA26R-lacZ and CAG-Td-tomato, were each crossed with *Asic4*^{CreERT2} mice. Double transgenic animals 12–16 weeks old were used for tamoxifen induction. Mice received daily intraperitoneal injection of 2 mg tamoxifen for seven consecutive days and food chow was replaced with a special diet containing tamoxifen citrate (400 mg/kg) purchased from the Harlan laboratory (Fig. 2A). Animals were killed 7 days after 7-day tamoxifen treatment and tissues were taken for X-gal staining or immunofluorescence. For prenatal embryo induction, pregnant dams at the E16.5–18.5 stage received two daily 2 mg tamoxifen injections, and pups were collected at birth for X-gal staining of tissue.

X-gal staining and immunohistochemistry

To analyse the temporal and spatial pattern of tamoxifen-induced Cre recombination, heterozygotes were crossed with the ROSA26R-lacZ or CAG-Td-tomato Cre reporter mice. After tamoxifen induction, mice were perfused with 25 mL ice-cold phosphate-buffered saline (PBS) followed by 25 mL 4% paraformaldehyde (PFA) in PBS. Tissues were removed and post-fixed in 4% PFA at 4 °C for 6–8 h. For whole-mount X-gal staining, the base of the skull containing the pituitary gland, part of the optic nerve and the trigeminal ganglions were soaked in the X-gal solution (NaCl, 0.15 M; $K_3Fe(CN)_6$, 3.5 mM; $K_4Fe(CN)_6$, 3.5 mM; PB, pH 7.4, 0.01 M; $MgCl_2$, 1 mM; chloroquine, 0.3 M; sodium deoxycholate, 0.01%; NP-40, 0.2%; and X-gal, 1 mg/mL) at 37 °C for 6 h. For perinatal X-gal staining, cryosections 16 μm thick were taken from P0 pups and mounted on gelatin-coated slides. Samples were soaked in the X-gal solution at 37 °C for 6 h and counterstained with Neutral Red. For immunofluorescence, cryosections 16 μm thick were taken from mouse brains and spinal cords, dried at room temperature for 10 min, then post-fixed in 4% PFA for 10 min. Sections were washed three times with PBS+0.1% Triton X-100 (PBST) and blocked for 1 h at room temperature in PBST containing 3% bovine serum albumin and 5% normal serum of the second antibody host. Primary antibodies were diluted in blocking solution and incubated overnight at 4 °C. Sections were then washed three times with PBST and incubated for 1 h at room temperature with secondary antibodies (1:400). Primary antibodies and their titers were as follows: rabbit-anti-parvalbumin (Pv) (GenTex, Irvin, CA, USA; 1:300); mouse-anti-calbindin (CB) (Swant, Marly, Switzerland; 1:300); rabbit-anti-NG2 (Millipore, Darmstadt, Germany; 1:300); mouse-anti-calretinin (CR) (Swant; 1:300); rabbit-anti-vasoactive intestinal peptide (VIP) (Immunostar, Hudson, WI, USA; 1:500); rabbit-anti-neuropeptide Y (NPY) (Immunostar; 1: 500); rat-anti-somatostatin (SOM) (Millipore; 1:500); and rabbit-anti-Pax6 (Millipore; 1:500).

Body composition test

Body composition of mice was measured by use of the Whole Body Composition Analyzer (Bruker, Karlsruhe, Germany). We measured fat, free body fluid and lean tissue by Time Domain Nuclear Magnetic Resonance Spectroscopy (Minispec LF50, Bruker).

Home-cage activity test

We used an automatic imaging recognition system, HomeCageScan 3.0 software (Clever System, Reston, VA, USA), to monitor and analyse mouse behaviors for 48 h in the home cage with a 12-h dark/light cycle. Positions of the rodent body, including the head, mouth, ears, upper/lower back, forelimb/hindlimb, abdomen and tail, were used to analyse the relationship between a certain behavior and the position of these body parts. HomeCageScan 3.0 can detect

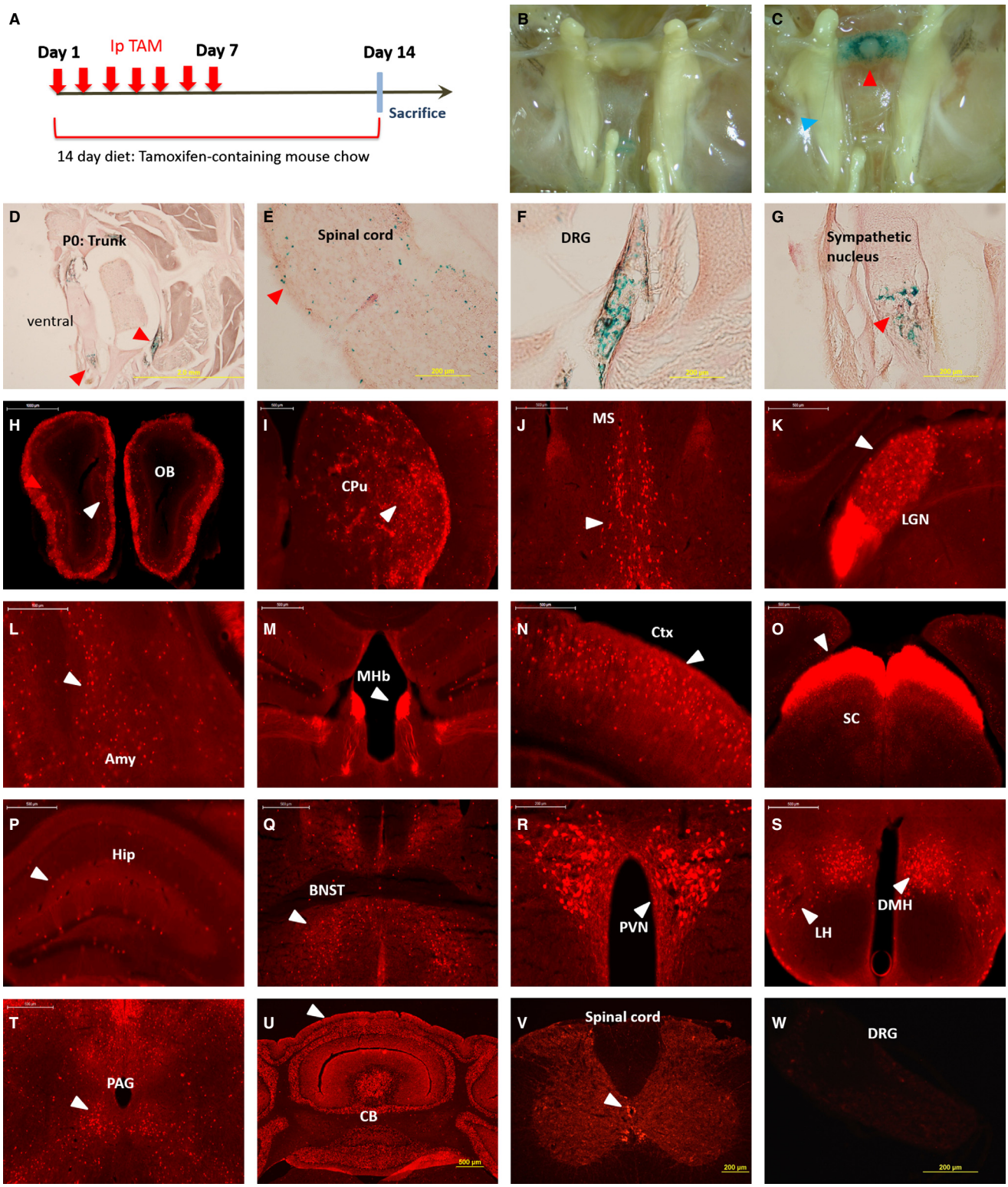

FIG. 2. The expression of ASIC4 in the nervous system was mapped at the cellular level by using inducible-Cre/loxP technology. (A) Schematic diagram of the strategy of tamoxifen-induced Cre recombination for ASIC4 mapping. After crossing with transgenic Cre-reporter mouse line ROSA26R-lacZ or CAG-Td-tomato, double transgenic mice were treated with tamoxifen (2 mg/day) by intraperitoneal injection for 7 days, and food chow was replaced with a special diet containing tamoxifen citrate for 14 days. (B and C) Whole-mount X-gal staining detected $CreERT^2$-mediated reporter LacZ-expression in the pituitary gland (red arrowhead) but not trigeminal ganglia (blue arrowhead) in adult $Asic4^{CreERT2/CreERT2}$::ROSA26R-lacZ mice. (D–G) Prenatal expression of ASIC4 in the DRG and sympathetic ganglia (arrowheads) detected at E16.5–18.5 with tamoxifen (2 mg/day) treatment of pregnant mothers 2 days before birth. (H–W) In adult mice, ASIC4 was expressed in many brain regions (arrowheads) including the granular layer of the olfactory bulb (OB), caudate nucleus (CPu), medial septum (MS), lateral geniculate nucleus (LGN), amygdala (Amy), medial habenular (MHb), entire cortex (Ctx), superior colliculus (SC), hippocampus (Hip), bed nucleus of stria terminalis (BNST), paraventricular nucleus (PVN), dorsomedial hypothalamic nucleus (DMH), lateral hypothalamus (LH), periaqueductal gray (PAG), cerebellum (CB) and spinal cord but not DRG.

eating, drinking, walking, rearing up, resting, awakening, twitching, grooming and hanging with high accuracy.

Rotarod and nociception tests

The rotarod test was performed with a PC software-controlled mouse Rota-Rod (3-cm diameter; Ugo Basile, Varese, Italy). Three trials of training were started at 0 rpm for 60 s and then 4 rpm for 60 s. Mice were tested at accelerating speeds from 4 to 40 rpm over 300 s, and the latency (in s) and speeds of the rod (in rpm) when the mouse fell were recorded. For the electronic von Frey test, the mouse was placed in an acrylic box on the wire mesh for a 2-h habituation. A Rigid Tip (0.025-cm tungsten electrode) connected to the Anesthesiometer (IITC Life Science, Woodland Hills, CA, USA) was used to poke the mouse hind paw. Mechanical threshold (in g) was measured when the withdrawal response appeared. Both the left and right paw were measured 10 times and averaged to reduce errors. Tail flick and hot plate tests involved use of the Hot/Cold Plate 35100 and Tail Flick Unit 37360 (Ugo Basile), respectively. In the hot-plate test, the thermal nociceptive threshold (one trial, latency in seconds) was measured when the tested mouse showed signs of lifting or licking hind paws or jumping after placement on the 55 $\pm$ 0.1 °C metal plate. In the tail-flick test, infrared radiant heat generated from a 50-W bulb was applied to the subject's tail (2–3 cm from the end) and the latency of tail flick was recorded once.

Innate fear to predator odor and contextual fear conditioning test

To measure freezing behavior, each mouse was placed in a near-infrared video conditioning chamber (Med Associates, St Albans, VT, USA) and allowed to habituate for 3 min. In the predator-odor induced fear test, mice were placed into the chamber and 20 μL 2,4,5-trimethylthiazoline (TMT; Phero Tech, Delta, BC, Canada), a synthetic analog of red fox feces, was applied to a cotton ball and placed in a small beaker underneath the floor of the chamber (Coryell *et al.*, 2007). In the contextual fear training session, five foot-shocks (1 s, 0.75 mA) were delivered to the floor grid with an inter-shock interval of 1 min. Each mouse was returned to the home cage immediately after the training and, 24 h later, placed back in the conditioning chamber for measuring freezing behavior for 5 min. Freezing response was defined as an absence of movement other than respiration and was recorded by use of video-tracking software (Med Associates) (Chao *et al.*, 2013).

Anxiety tests

The open field (OF) test was performed in a 48 $\times$ 48 $\times$ 48-cm, 4-wall chamber with 100 lx illumination. The mouse was released into the corner of the arena and allowed to freely explore for 20 min. In the elevated-plus maze (EPM) test, an apparatus with two open arms (30 $\times$ 5 cm, with 1-cm ledges) and two closed arms (30 $\times$ 5 cm, with 15-cm walls) was used. The maze was elevated to a height of 50 cm above the floor during the task. The movement traces of each mouse in these two tasks was recorded and the time each mouse stayed in the center area (16 $\times$ 16 cm) in the OF and in the open arm in the EPM was analysed with use of TopScan (Clever System) (Wu *et al.*, 2010).

Kainic acid-induced seizure

The behavior of each mouse was videotaped for 60 min after intraperitoneal injection of 15 mg/kg (low dose) or 30 mg/kg (high dose) kainic acid (Ziemann *et al.*, 2008). A double-blinded observer judged the Racine score of seizure symptoms every 10 min. The Racine score is defined as 0, no response; 1, reduced locomotion; 2, rigidity; 3, repetitive movements; 4, rearing with clonus; 5, loss of posture; 6, status epilepticus and death.

Amphetamine-induced hyperlocomotion and CPP test

The stimulating and rewarding effect of amphetamine in mice was evaluated in a 22 $\times$ 22 $\times$ 30-cm two-chamber acrylic cage. One chamber had a strip-wire floor with dot-painted walls and the other chamber had twill mesh and stripe-painted walls. The unbiased conditioning procedure was adopted and all subjects were randomly assigned to paired drug to one of the two chambers. The CPP task lasted for 10 consecutive days and consisted of three phases: habituation, drug-pairing and preference test. On day 1, the mouse was placed in the apparatus to explore freely for 15 min with the barrier between the two chambers opened. On days 2, 4, 6 and 8, the mouse received an intraperitoneal drug injection and was confined to the drug-paired chamber for 30 min; on days 3, 5, 7 and 9, the mouse received a saline injection and was confined to the saline-paired chamber for 30 min. On day 10, the drug-free animal was given free access to the two chambers and the time spent in each chamber was recorded for 15 min. The moving traces for each mouse in the three sessions were recorded and analysed with use of the TopScan (Clever System) system. Briefly, the arena without mouse was first calibrated as background with white paper under the mesh, and then mouse was placed in the chamber and the software automatically identified the center of the whole body. Horizontal travelling distance (in cm) was calculated for each 5-min interval and used as an index of locomotion. The times (in s) each mouse stayed in each chamber over the 15 min in both the habituation (pretest) and CPP test (posttest) were calculated as an index of preference score.

Cookie-finding test

The cookie test was to evaluate the olfactory function in mice and performed as previously described (Dawson *et al.*, 2005). Briefly, mice at the age of 14–18 weeks were food-restricted during the whole cookie-test session, when they got free access to mouse chow for only 1 hour after the behavioral test in the early dark phase. On the first habituation day, mice were moved to a glass tank (13 $\times$ 27 $\times$ 48 cm) and a piece of cookie ~50 mg (ACE, milk flavor, Chu Jung Food Co., Taiwan) was placed on the surface of the 3-cm-deep sawdust. Mice approached and ate the cookie immediately. After the mouse had finished eating it was placed back in its homecage. In the next three consecutive testing days, each mouse learned to locate the cookie that was randomly buried 1 cm beneath the surface of the sawdust. The experimenter recorded the time (in s) each mouse needed to find the cookie. A maximum time of 300s was recorded if the mouse did not locate the cookie within 5 min.

Statistical analysis

Data in all figures are presented as mean $\pm$ SEM. Statistical comparisons involved use of SigmaState 3.5. (Systat Software Inc., San Jose, CA, USA) Unless otherwise specified, analysis involved Student's *t*-test or ANOVA, with the Holm–Sidak method used for *post hoc* analysis; otherwise the non-parametric Mann–Whitney test was used. $P < 0.05$ was considered statistically significant.

Results

ASIC4-KO/Cre-ERT^2-knockin mouse

The targeting vector to generate *Asic4*-KO contained a 1.7-kb 5′-arm, 4.3-kb 3′-arm, CreERT^2 cDNA (subcloned from the Pv-Cre-ERT^2-knockin mouse, Jackson lab; stock no. 010777) and the positive selection gene 'floxed-pGK-neo cassette' (Fig. 1A). After two trials of ES-cell electroporation, 346 ES clones were obtained and screened for homologous recombination by long-range PCR with 5′-arm flanking primers and Southern blot hybridisation with a 3′-arm flanking probe. One ES cell clone, no. 63, showing correct homologous recombination in both arms, was chosen for blastocyst microinjection (Fig. 1B and C). In the targeted allele, exon1 of *Accn4*, a fragment of 0.8 kb after the translation start site was deleted and replaced with the cDNA of CreERT^2. Chimeras were crossed to WT C57BL/6J mice to generate F1 mice. After germ-line transmission, the floxed pGK-neo cassette was removed by crossing to protamine-Cre-deleter mice. Male F2 offspring bearing both the KO allele and the protamine-Cre allele were then crossed to WT female C57BL/6J mice for the F3 generation. Thereafter, animals were screened for genotype by PCR (Fig. 1D). ASIC4 homozygous KOs were viable and fertile, and displayed no obvious defects in appearance. To confirm the elimination of ASIC4 transcripts, we examined samples of brain regions from adult *Asic4*$^{+/+}$ and *Asic4*$^{-/-}$ mice by real-time RT-PCR. In the WT, ASIC4 transcripts were detectable in every brain region selected and were most abundant in the pituitary gland but barely detectable in the DRG. The expression of ASIC4 transcripts in these brain regions was eliminated in the KO samples (Fig. 1E). Next, we examined whether ASIC4-KO might alter the expression of other ASIC subtypes because of possible compensation effects. The transcript levels of ASIC1a (Fig. 1F) and ASIC3 (Fig. 1G) did not obviously differ between *Asic4*$^{-/-}$ and WT littermates.

Expression of ASIC4 in the nervous system

Because CreERT^2 was knocked into the ASIC4 locus, we could map the expression of ASIC4 on a Cre-reporter mouse via tamoxifen-induced Cre-mediated DNA recombination. We thus designed a tamoxifen-induction paradigm and treated *Asic4*$^{CreERT2/CreERT2}$::ROSA26R-lacZ or *Asic4*$^{CreERT2/CreERT2}$::CAG-Td-tomato mice with tamoxifen for 14 days (Fig. 2A). We first examined the induction efficiency of CreERT^2-mediated DNA recombination by the whole-mount X-gal approach in *Asic4*$^{CreERT2/CreERT2}$::ROSA26R-lacZ mice. As expected, intense X-gal signal (ASIC4 expression) was detected in the pituitary gland of the mice, especially in the anterior and intermediate lobe but not trigeminal ganglia (TG) or control mice (Fig. 2B and C). The expression of ASIC4 in the pituitary gland but not the TG or DRG agreed with previous reports from human (Grunder *et al.*, 2000), rat (Akopian *et al.*, 2000) and mouse (Du *et al.*, 2014) samples. In the CNS, X-gal-positive signals were detected in many regions, including the olfactory bulb, cortex, hippocampus, amygdala, thalamus, hypothalamus, cerebellum and spinal cord but not adult DRG (data not shown). These results agreed with real-time RT-PCR data (Fig. 1E).

The expression of ASIC4 in the peripheral nervous system seems to be controversial because previous studies detected ASIC4 protein (Alvarez de la Rosa *et al.*, 2002) but only a small amount of mRNA (Macdonald *et al.*, 2001) in the rat DRG. Possible explanations for this difference might be tool sensitivity, species variation or some developmental control. We detected X-gal signals in DRG and sympathetic ganglion of neonatal mice at P0 when their pregnant mothers had been treated with tamoxifen, which suggests that ASIC4 was expressed in the peripheral nervous system during the embryonic stages (Fig. 2D–G). To provide a better resolution in characterising the identity of these ASIC4-expressing cells, we examined *Asic4*$^{CreERT2/CreERT2}$::CAG-Td-tomato mice in the later mapping studies. After the same tamoxifen induction (Fig. 2A), Td-tomato signals were detectable in the granular layer of the olfactory bulb, caudate–putamen, medial septum, lateral geniculate nucleus, amygdala, medial habenular nucleus, cortex, superior colliculus, dorsal and ventral hippocampus, bed nucleus of stria terminalis, paraventricular nucleus, dorsomedial hypothalamus, lateral hypothalamic nucleus, periaqueductal gray, granular layer of the cerebellum and central canal of the spinal cord but not DRG (Fig. 2H–W).

Colocalisation studies reveal ASIC4 expressed in neurons with immunoreactivity of CR and VIP as well as neural/glial antigen 2 cells in the CNS

We next aimed to determine the identity of the ASIC4-expressing cells. We examined whether ASIC4 signals were colocalised with specific cell markers in the cortex, amygdala and cerebellum, major brain areas showing high expression levels of ASIC1a, the principal ASIC subtype responding to acid signaling in the CNS (Ziemann *et al.*, 2009; Zeng *et al.*, 2013). In the cortex, the cell morphology, size and scattered distribution of these ASIC4-expressing cells suggested that they may be the cortical interneurons. Therefore, we used neurochemical markers such as Pv, SST, CB, CR, VIP and NPY to identify the major classes of cortical interneurons (Wonders & Anderson, 2006). Immunohistochemistry revealed that ASIC4-expressing cells in the cortex were colocalised with CR and VIP but not Pv, SST, CB or NPY (Fig. 3A–L). Three independent trials (eight sets of slides) of colocalisation studies suggested that, in the cortex, ~40% (217/540) and ~59% (321/540) of ASIC4-expressing cells were CR$^+$ and VIP$^+$ GABAergic interneurons, respectively. ASIC4 was expressed in ~23% (512/2228) of total CR$^+$ and ~65% (728/1121) of total VIP$^+$ neurons in the cortex. Cortical CR$^+$ interneurons can be divided into at least two populations: VIP$^+$–bipolar interneurons and SOM$^+$–Marttinotti-like interneurons (Cauli *et al.*, 2014). In mice, co-expression of CR and VIP in the cortex is ~ 35% (Xu *et al.*, 2010) and our data excluded the expression of ASIC4 in SOM$^+$–Marttinotti cells. To probe whether ASIC4 is expressed specifically in CR$^+$+VIP$^+$ cells, we performed double colocalisation staining and found that 21% (118/540) of ASIC4-expressing cells were CR$^+$ and VIP$^+$, 57% (302/540) were CR$^+$ or VIP$^+$ and ~ 22% (120/540) were neither CR$^+$ nor VIP$^+$ (Fig. 4A) Almost the same ratio of colocalisation between ASIC4 and CR/VIP was found in the amygdala (Fig. 4B).

The cell identity of the other 22% ASIC4-expressing cells was unknown. Previous studies of rats suggested that ASIC4 mRNA is expressed in cultured oligodendrocyte progenitor (OP) cells (Feldman *et al.*, 2008) and ASIC1a is highly expressed in NG2 cells, also known as OP cells (Lin *et al.*, 2010). We thus performed colocalisation studies with cell markers of astrocytes (glial fibrillary acidic protein; GFAP) and OP cells (NG2). A small proportion of ASIC4-expressing cells were NG2$^+$ polydendrocytes (Fig. 4C–E), but none were colocalised with GFAP (data not shown). The cell morphology of ASIC4-exprsssing cells in the cerebellum differed from that of cortical interneurons and NG2$^+$ OP cells. Colocalisation study revealed that they were Pax6$^+$ granular cells (Fig. 4F–H), the smallest neurons contributing to the parallel fibers in the cerebellar cortex.

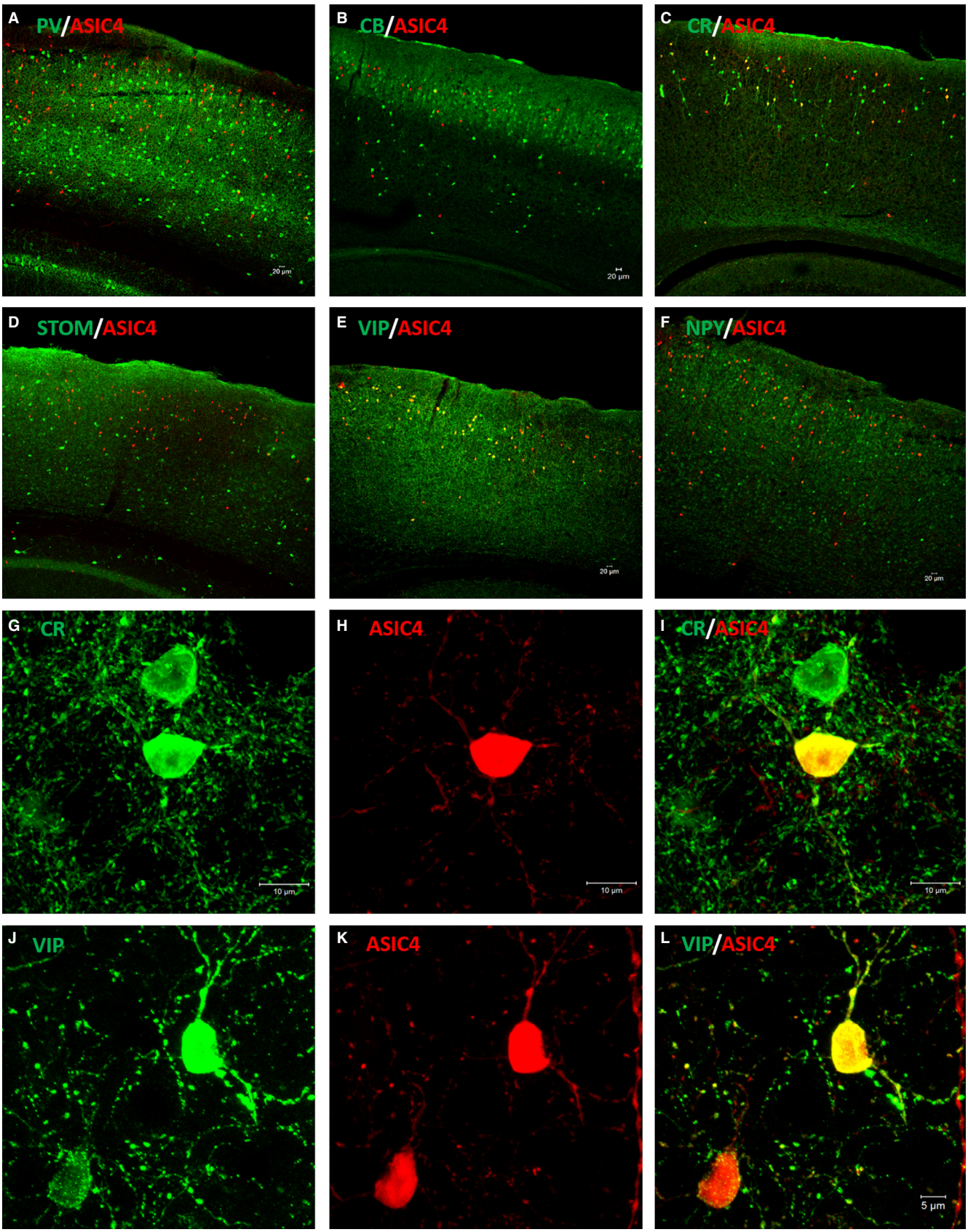

FIG. 3. ASIC4 colocalises with CR and VIP in subsets of cortex neurons. (A–F) Immunostaining with fluorescence microscopy to determine the cell identity of ASIC4-positive cells in the cortex region. Known cortical interneuron markers including Pv, CB, CR, SST, VIP and NPY were used to examine their colocalisation with Td-tomato signals. ASIC4 was specifically expressed in some CR- and VIP-positive interneurons. (G–I) High-magnification images of the colocalisation of ASIC4 and CR in the mouse cortex. (J–L) High-magnification images of the colocalisation of ASIC4 and VIP in the mouse cortex.

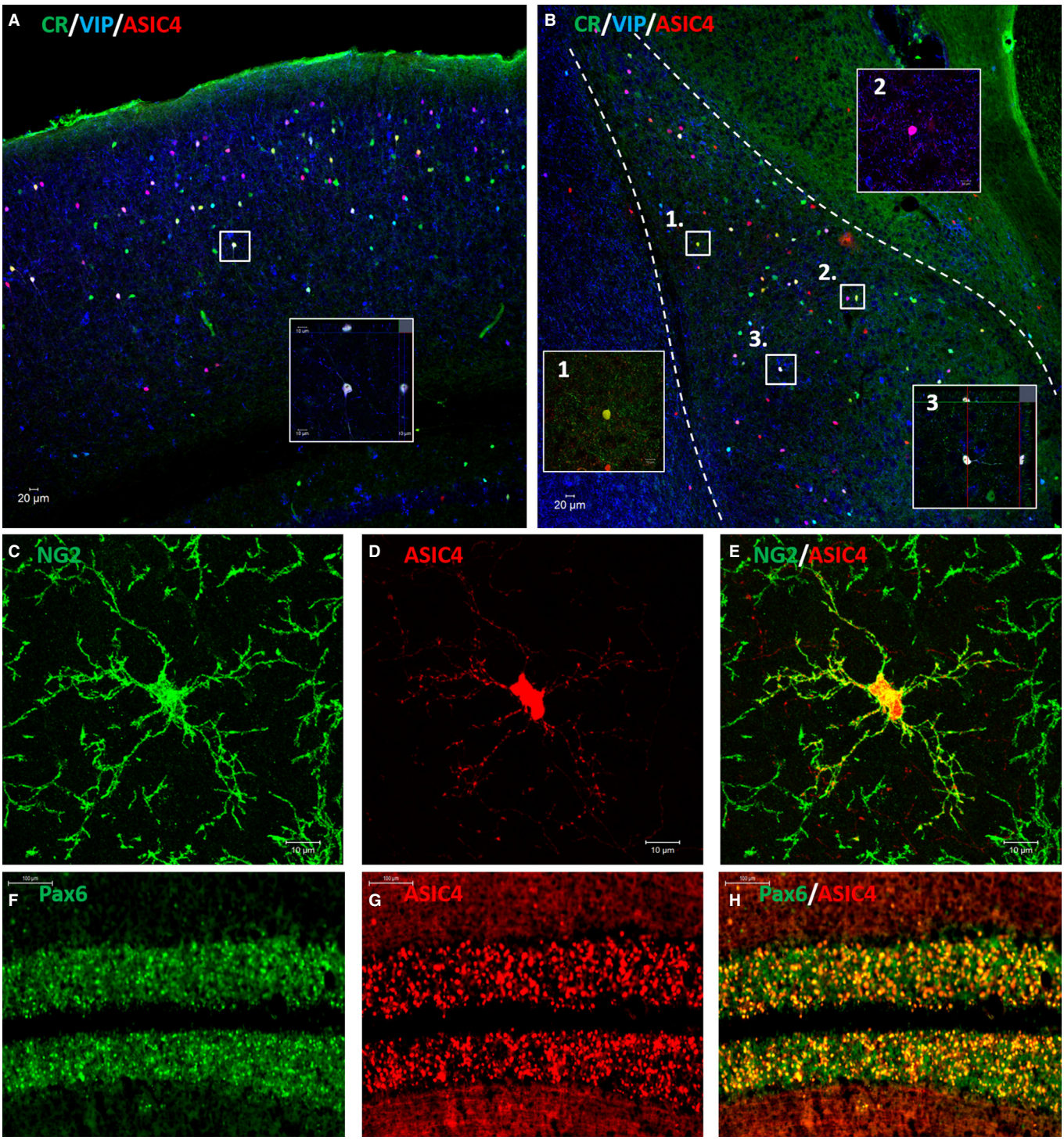

FIG. 4. ASIC4 is expressed in CR- and/or VIP-positive interneurons and NG2-positive cells in the cortex and amygdala and in the granular cells of the cerebellum. (A) In the cortex, double staining detected ASIC4 signals in some CR-positive-only cells (yellow), some VIP-positive-only cells (purple) and some cells which are CR- and VIP-positive (white) in the cortex. The inset square is a high-magnification image of a cell which is positive for ASIC4, CR and VIP. (B) Almost all ASIC4-positivity was detected in the CR-, VIP- or CR/VIP-positive interneurons in the amygdala. The three inset squares illustrate one ASIC4–CR-positive, one ASIC4–VIP-positive and one ASIC4–CR–VIP-positive cell in high magnification. (C–E) Some ASIC4 signals were detected in NG2-positive cells in the cortical regions. (F–H) In the cerebellum, ASIC4 was mainly expressed in the granular cell layers in view of the perfect colocalisation of Td-tomato and known marker Pax6.

ASIC4-KO mice showed normal body composition, home-cage activity, nociception and motor coordination

Asic4$^{-/-}$ mice showed normal growth rate (up to 16 weeks old) and normal appearance as compared with WT littermates. The expression pattern of ASIC4 in the CNS suggested that we screened the possible phenotype(s) of *Asic4*$^{-/-}$ mice. Because ASIC4 signals were abundant in the hypothalamus, the pituitary gland and the granular layer of the cerebellum, we first screened phenotypes related to these brain

functions. We tested (i) the body composition of fat, lean and free water, (ii) the home-cage activity for 48 h in a 12-hr light/dark cycle, (iii) the thermal and mechanical thresholds in nociception and (iv) motor coordination ability in the rotarod test. WT and *Asic4*$^{-/-}$ mice did not differ in body composition and home-cage activity (Tables 1 and 2). In the 48-h home-cage activity, some well defined behaviors such as resting (Fig. 5A) and drinking (Fig. 5B) showed a distinct pattern within the light and the dark phases, which can be used as an index to probe possible variation in the circadian rhythm. *Asic4*$^{-/-}$ mice showed normal resting episodes in the 2-day light phase, with a significant effect of hour ($F_{11,198}$ = 3.65, P < 0.01) but not genotype ($F_{1,198}$ = 0.48, P = 0.49) or their interaction ($F_{11,198}$ = 1.23, P = 0.27) (Fig. 5A; Tables 1 and 2). *Asic4*$^{-/-}$ mice had normal drinking episodes in the dark phase, with a significant effect of hour ($F_{11,198}$ = 3.72, P < 0.01) but not genotype ($F_{1,198}$ = 1.80, P = 0.20) or their interaction ($F_{11,198}$ = 1.56, P = 0.14) (Fig. 5B). These results ruled out the possible involvement of ASIC4 in modulating circadian activity *in vivo*. In the nociception tests, *Asic4*$^{-/-}$ mice had a normal mechanical withdrawal threshold in the von Frey test (t_{18} = 0.85, P = 0.41, Fig. 5C), tail flick test (t_{18} = 0.62, P = 0.54, Fig. 5D) and hotplate test (t_{18} = 0.90, P = 0.38, Fig. 5E).

In the cerebellum, ASIC4 was expressed selectively in granular cells in every lobule. Previous study suggested an essential role for these cells in motor learning (Galliano *et al.*, 2013). Therefore, we screened a possible motor-learning phenotype of *Asic4*$^{-/-}$ mice in the rotarod task. For 'the latency to fall', we found a significant effect of training ($F_{2,36}$ = 4.66, P < 0.05) but not genotype ($F_{1,36}$ = 0.193, P = 0.67) or their interaction ($F_{2,36}$ = 0.15, P = 0.86) (Fig. 5F). In the 'maximum speeds used', we found a significant effect of training ($F_{2,36}$ = 4.46, P < 0.05) but not genotype ($F_{1,36}$ = 0.18, P = 0.68) or their interaction ($F_{2,36}$ = 0.10, P = 0.91) (Fig. 5G). Therefore, ASIC4 in the granule cells of the cerebellum did not play a role in motor learning.

TABLE 1. Phenotyping for ASIC4-KO: normal body composition

			Statistics		
Body composition	Wildtype	ASIC4-KO		t_{18}	P
Body weight (g)	29.12 ± 0.50	28.46 ± 0.56	NS	0.62	0.54
Fat (g)	3.50 ± 0.23	3.38 ± 0.24	NS	0.35	0.73
Lean (g)	21.97 ± 0.27	21.21 ± 0.69	NS	1.04	0.32
Free fluid (g)	2.29 ± 0.05	2.23 ± 0.08	NS	0.65	0.53
Total water (g)	19.87 ± 0.26	19.17 ± 0.63	NS	1.02	0.32

Data are mean ± SEM; n = 10 for each group. NS, no significant difference.

ASIC4-KO and ASIC1a-KO showed opposite phenotypes only in innate fear to TMT and anxiety-like behaviors

We next pursued phenotyping assays related to ASIC1a function. Our working hypothesis was that *Asic4*$^{-/-}$ mice might have opposite phenotypes to *Asic1a*$^{-/-}$ mice because ASIC4 could counteract ASIC1a activity on the cell membrane (Donier *et al.*, 2008). We examined four important phenotypes of ASIC1a mutants: (i) impairment in electric shock-evoked fear-conditioning task (Wemmie *et al.*, 2003; Coryell *et al.*, 2008; Gregoire & Matricon, 2009); (ii) increased severity in kainic acid-induced seizure (Ziemann *et al.*, 2008); (iii) impaired innate fear response to TMT and reduced anxiety-like behavior in the OF and EPM (Coryell *et al.*, 2007; Price *et al.*, 2014); and (iv) increased craving potential to psychostimulant cocaine (Kreple *et al.*, 2014). We screened these behaviors in *Asic4*$^{-/-}$ mice with their WT controls and *Asic1a*$^{-/-}$ mice. Consistent with previous studies, *Asic1a*$^{-/-}$ mice showed an impaired freezing response (unconditioned response) to electric shock (unconditioned stimulus) during the training session as compared with the WT, with a significant effect of genotype ($F_{2,72}$ = 12.67, P < 0.01) and training ($F_{4,72}$ = 17.60, P < 0.01) but not their interaction ($F_{8,72}$ = 0.27, P = 0.97) (Fig. 6A). *Post hoc* comparison of genotypes indicated a significant difference between the WT and *Asic1a*$^{-/-}$ (t = 4.85, P < 0.01), *Asic4*$^{-/-}$ and *Asic1a*$^{-/-}$ (t = 3.78, P < 0.01) but not the WT and *Asic4*$^{-/-}$ (t = 0.72, P = 0.48). In the retention test 24 h later, only *Asic1a*$^{-/-}$ mice showed impeded conditioned freezing response to the same chamber context. We found a significant effect of genotype ($F_{2,18}$ = 19.53, P < 0.01) and *post hoc* comparison revealed a significant difference between the WT and *Asic1a*$^{-/-}$ (t = 6.12, P < 0.01) and between *Asic4*$^{-/-}$ and *Asic1a*$^{-/-}$ (t = 4.42, P < 0.01) but not between the WT and *Asic4*$^{-/-}$ (t = 1.27, P = 0.22) (Fig. 6B). Unlike *Asic1a*$^{-/-}$ mice, *Asic4*$^{-/-}$ mice showed normal unconditioned and conditioned fear responses to electrical foot-shock and test chamber, respectively. In the kainic acid-induced seizure response, *Asic1a*$^{-/-}$ and their WT littermates were treated with low dose (15 mg/kg) kainic acid for recording seizure severity in Racine scores for 1 h. Consistent with previous reports (Ziemann *et al.*, 2008), seizure scores were higher for *Asic1a*$^{-/-}$ than WT mice. We found a significant effect of genotype ($F_{1,65}$ = 12.41, P < 0.01), session ($F_{5,65}$ = 9.34, P < 0.01) and their interaction ($F_{5,65}$ = 4.71, P < 0.01). *Post hoc* comparison revealed significant difference by genotype in sessions 2–6 but not session 1 (Fig. 6C). This result correlates well with ASIC1a playing an important role in seizure termination but not seizure initiation (Ziemann *et al.*, 2008). Also, ~42.8% (3/7) of *Asic1a*$^{-/-}$ mice died but no (0/8) WT mice died. In contrast to *Asic1a*$^{-/-}$, the seizure scores of

TABLE 2. Phenotyping for ASIC4-KO: circadian home-cage activity

					Statistics					
	Wildtype		ASIC4-KO		Genotype		L/D cycle		Interaction	
Home cage scan	Day	Night	Day	Night	F	P	F	P	F	P
Dist. travelled (m)	5.84 ± 0.55	23.99 ± 2.31	4.39 ± 0.67	20.36 ± 2.49	1.58	0.23	105.75	0.01	0.44	0.52
Resting	2347.14 ± 44.10	984.92 ± 63.42	2471.69 ± 66.84	982.62 ± 87.50	0.72	0.41	417.61	< 0.01	0.83	0.38
Drinking (event)	7.95 ± 0.72	34.90 ± 3.08	6.05 ± 1.09	35.81 ± 3.82	0.03	0.86	116.19	< 0.01	0.284	0.60
Feeding (event)	112.69 ± 7.50	664.63 ± 49.41	100.04 ± 15.95	418.64 ± 73.69	0.001	0.97	50.64	< 0.01	0.06	0.81
Grooming	582.53 ± 30.99	648.72 ± 48.97	498.65 ± 39.86	808.77 ± 60.07	1.88	0.19	66.98	< 0.01	0.02	0.89
Hanging	44.63 ± 10.29	343.55 ± 46.23	42.12 ± 19.68	356.50 ± 86.55	0.01	0.93	40.66	< 0.01	0.03	0.87
Rearing up	15.37 ± 2.70	59.63 ± 8.92	12.26 ± 4.25	46.19 ± 7.88	0.96	0.34	66.63	< 0.01	1.16	0.30
Walking	47.45 ± 4.26	105.01 ± 7.93	35.34 ± 4.59	105.02 ± 7.40	0.64	0.44	130.41	< 0.01	1.18	0.29

Data are mean ± SEM; n = 10 for each group.

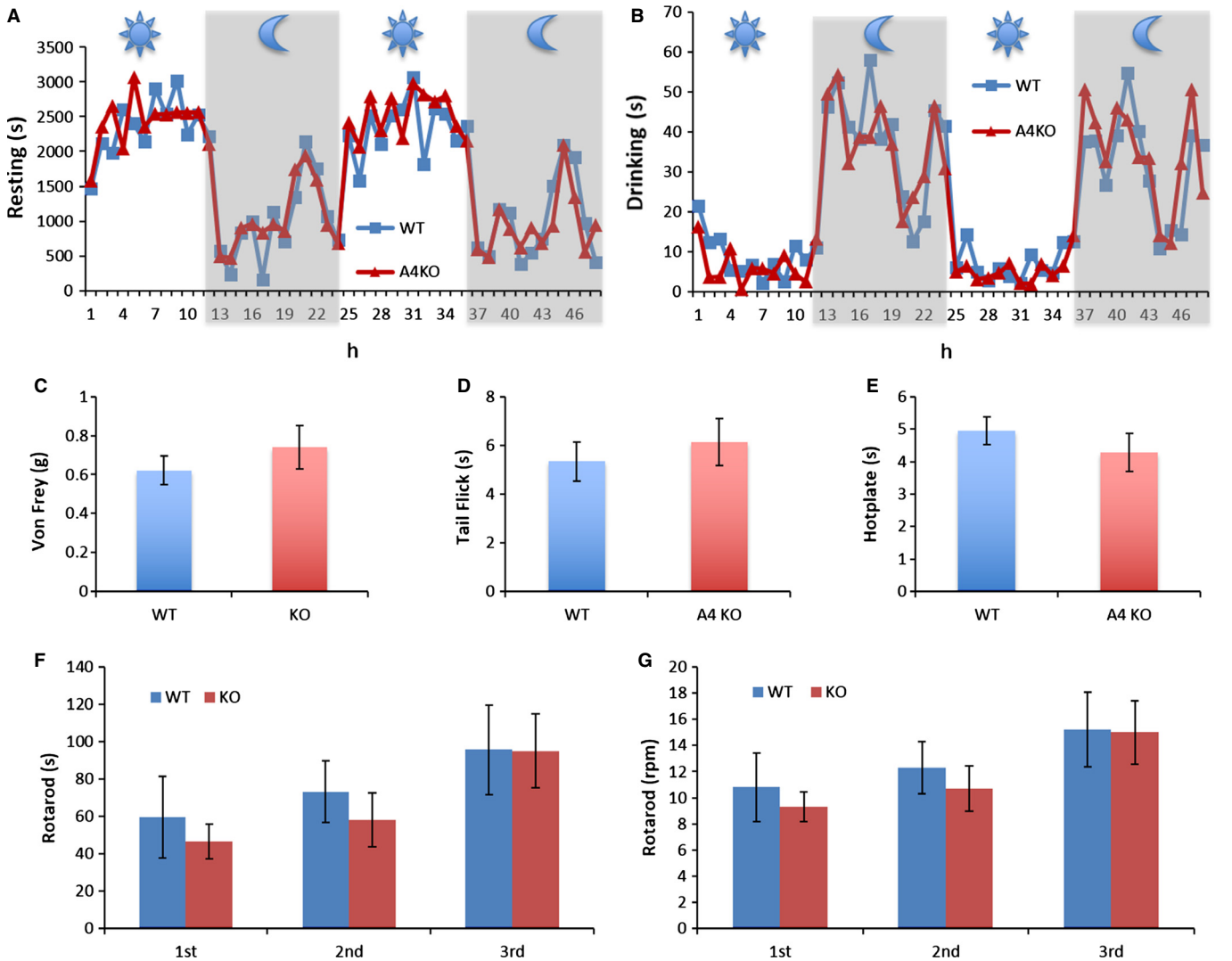

FIG. 5. ASIC4 mutants demonstrated normal home-cage activity, nociceptive sensitivity and motor learning capacity. (A) In the 48-h home-cage activity recording, distinct behavior events were sorted and recorded by image recognition software. Resting behavior predominantly appears in the light phase in mice and thus provides a suitable index for verifying the circadian-related phenotypes between *Asic4*$^{-/-}$ (n = 10) and wildtype (n = 10) mice. (B) Another dichroic behavior, drinking, predominantly appears in the dark phase in mice (n = 10 for each genotype). (C) Mechanical nociception by von Frey test (n = 10 for each genotype). (D and E) Thermal nociception by both tail-flick and the hotplate tests (n = 10 for each genotype). (F and G) Motor learning ability assessed in the three-trial rotarod test (n = 10 for each genotype).

Asic4$^{-/-}$ and WT mice were indistinguishable at the same dose (genotype effect: $F_{1,70}$ = 0.01, P = 0.92; session: $F_{5,70}$ = 2.54, P < 0.05; and interaction: $F_{5,70}$ = 0.52, P = 0.76; Fig. 6D) or the higher dose (30 mg/kg) of kainic acid treatment (genotype effect: $F_{1,70}$ = 0.01, P = 0.92; session: $F_{5,70}$ = 2.54, P < 0.05; and interaction: $F_{5,70}$ = 0.52, P = 0.76; Fig. 6E).

Ziemann *et al.* (2008) attributed the seizure termination effect of ASIC1a to the acidosis-evoked activation of inhibitory GABAergic

FIG. 6. Behavioral phenotyping of *Asic4*$^{-/-}$ mice focusing on *Asic1a*$^{-/-}$ phenotypes. (A) *Asic1a*$^{-/-}$ mice are known to display learning and memory deficits in the contextual fear conditioning test. In the acquisition phase, mice showed little freezing with the first 3-min habituation (Hab) and subsequent five consecutive electrical shocks delivered at 1-min intervals. Compared with WT (n = 9) and *Asic4*$^{-/-}$ (n = 6), *Asic1a*$^{-/-}$ (n = 6) mice showed impairment in displaying a proper unconditioned freezing response. (B) In the retention phase 24 hr later, mice were placed back in the same conditioning chamber and recorded for conditioned freezing response for 5 min. (C) Kainic acid-induced seizure severity. Mice (n = 7 for *Asic1a*$^{-/-}$ and n = 8 for WT) received kainic acid (15 mg/kg) by intraperitoneal injection and were recorded for Racine score for the following 60 min. (D and E) Kainic acid-induced seizure severity with low dose (15 mg/kg; n = 8 for each group) or high dose (30 mg/kg; n = 10 for each group). (F) Innate fear response measured for 5 min when mice were exposed to the odor of predator (20 µl TMT, on cotton). Compared with WT (n = 18), *Asic1a*$^{-/-}$ mice (n = 10) showed less while *Asic4*$^{-/-}$ mice (n = 10) showed more freezing behavior in this condition. (G) In the cookie-finding test, time (in s) to locate the flavored cookie randomly buried in the sawdust was used as an index of olfaction. WT (n = 10), *Asic1a*$^{-/-}$ (n = 6) and *Asic4*$^{-/-}$ (n = 8) mice showed similar performance and progress in three consecutive test days. (H and I) State of anxiety assessed in mice using the OF and the EPM tests. (H) In the OF test, time (and frequency) for each mouse to come across or stay in the center area recorded as an index of anxiety-like behavior. *Asic1a*$^{-/-}$ mice (n = 10) showed more while *Asic4*$^{-/-}$ mice (n = 10) stayed less time than WT (n = 10) in the center area, indicating lower and a higher anxiety levels respectively. (I) In the EPM, time (and frequency) for each mouse to stay in the open arm was recorded. *Asic1a*$^{-/-}$ mice (n = 10) spent more time while *Asic4*$^{-/-}$ mice (n = 10) spent less time in the open arm than did WT (n = 10), which indicates lower and higher anxiety levels respectively. *P < 0.05, **P < 0.01 *Asic1a*$^{-/-}$ vs. WT; $^{\#\#}P$ < 0.01 *Asic1a*$^{-/-}$ vs. *Asic4*$^{-/-}$; $^{\$}P$ < 0.05, $^{\$\$}P$ < 0.01 WT vs. *Asic4*$^{-/-}$.

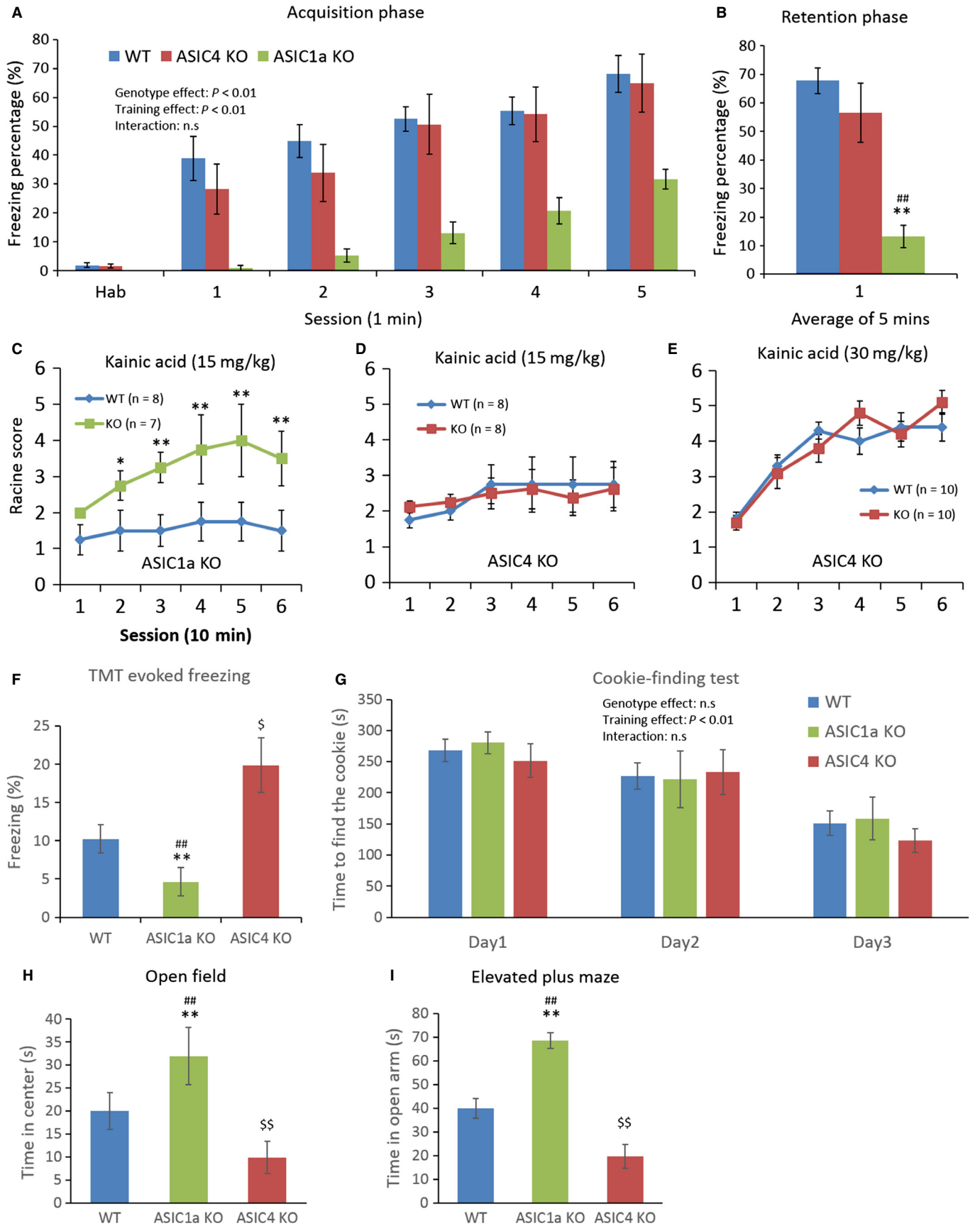

interneurons and, combined with our mapping results, we concluded that ASIC4 in CR/VIP-positive interneurons (or NG2-positive OP cells) were not involved in sensing synaptic acidosis upon seizure disturbance. The possible modulatory role of ASIC4 on ASIC1a first appeared in the test of TMT-induced innate fear response. As compared with WT controls, *Asic1a*$^{-/-}$ mice showed a decreased freezing response whereas *Asic4*$^{-/-}$ mice showed an increased freezing response in the 5-min exposure time (genotype effect: $F_{2,35} = 7.57$, $P < 0.01$), and *post hoc* comparisons revealed a significant difference between WT and *Asic1a*$^{-/-}$ (t = 2.74, $P < 0.01$), *Asic4*$^{-/-}$ and *Asic1a*$^{-/-}$ (t = 3.83, $P < 0.01$) and WT and *Asic4*$^{-/-}$ (t = 1.69, $P < 0.05$) (Fig. 6F). This result was encouraging because for the first time an *Asic4*$^{-/-}$ phenotype fulfilled the hypothesis that ASIC4 might counteract the activity of ASIC1a *in vivo*. *Asic4*$^{-/-}$ mice showed a normal fear response to electrical shock but an elevated fear response to TMT. The innate fear responses elicited by the odor of the predator (olfaction) and the electric shock (nociception) are possibly mediated by different neuronal mechanisms, and ASIC4 is only involved in the control of olfaction-mediated but not nociception-mediated fear responses. To rule out a possible olfactory deficit that might change the detection sensitivity of TMT and confound the interpretation of opposite innate fear phenotype in ASIC1a-KOs and ASIC4-KOs, we performed cookie-finding tests in these mice. In three consecutive testing days, all mice (WT, *Asic1a*$^{-/-}$ and *Asic4*$^{-/-}$) learned to locate the cookie that was randomly buried in the sawdust. Two-way ANOVA with repeated measurement indicated significant difference of training day ($F_{2,42} = 12.96$, $P < 0.01$), but not genotype ($F_{2,42} = 0.27$, $P = 0.77$) or interaction ($F_{4,42} = 0.18$, $P = 0.95$). For effect of training day, *post hoc* comparison revealed a significant difference between Day 1 vs. Day 3 (t = 4.99, $P < 0.01$) and Day 2 vs. Day 3 (t = 3.38, $P < 0.01$) but not Day 1 vs. Day 2 (t = 1.60, $P = 0.12$), indicating that all mice learned to locate the cookie with progress on the third day of training (Fig. 6G). We concluded that the olfactory function was normal, at least in the detection of the smell of flavor food, in *Asic1a*$^{-/-}$ and *Asic4*$^{-/-}$ mice. That the odor of predator evokes innate freezing responses less in *Asic1a*$^{-/-}$ but more in *Asic4*$^{-/-}$ cannot be explained by sensitivity differences in olfaction. Also, the amygdala circuit is not necessary in this kind of innate fear and this innate freezing response is disrupted after ablation of the olfactory bulb but not after deafferentation of the trigeminal input (Rosen *et al.*, 2008; Ayers *et al.*, 2013).

Asic4$^{-/-}$ mice also showed opposite phenotypes to *Asic1a*$^{-/-}$ mice in anxiety levels in the OF test, with a significant effect on center zone entry by genotype ($F_{2,29} = 48.21$, $P < 0.01$); *post hoc* comparisons indicated a significant difference between the WT and *Asic1a*$^{-/-}$ (t = 4.52, $P < 0.01$), the *Asic4*$^{-/-}$ and *Asic1a*$^{-/-}$ (t = 9.81, $P < 0.01$), and the WT and *Asic4*$^{-/-}$ (t = 5.29, $P < 0.01$) (Fig. 6H). In the EPM test we found a significant effect, on staying in the open arm, of genotype ($F_{2,29} = 24.73$, $P < 0.01$); *post hoc* comparisons indicated significant differences between the WT and *Asic1a*$^{-/-}$ (t = 4.11, $P < 0.01$), *Asic4*$^{-/-}$ and *Asic1a*$^{-/-}$ (t = 7.00, $P < 0.01$) and the WT and *Asic4*$^{-/-}$ (t = 2.89, $P < 0.01$) (Fig. 6I). Thus, *Asic1a*$^{-/-}$ mice could not demonstrate proper fear or anxiety, but *Asic4*$^{-/-}$ mice had problems suppressing exaggerated fear or anxiety under threatening situations.

ASIC1a-KO but not ASIC4-KO showed phenotypes in amphetamine CPP

ASIC4 is expressed in the striatum (Fig. 2I), a brain region with the strongest expression of dopamine transporter, the endogenous target for psychostimulant drugs such as cocaine and amphetamine. With cocaine the hyperlocomotion effect is lower (Jiang *et al.*, 2013) but the rewarding effect is higher (Kreple *et al.*, 2014) in *Asic1a*$^{-/-}$ than WT mice. We screened for possible phenotypes in *Asic4*$^{-/-}$ mice using the amphetamine-induced CPP paradigm. CPP has advantages in assessing three effects of a psychostimulant in the same task: (i) acute hyperlocomotion effect derived from the first trial of drug-pairing; (ii) behavioral sensitisation effect measured from the locomotor activity during four consecutive drug-pairing treatments; and (iii) rewarding effect assessed in the final drug-free, barrier-open, free exploration in two drug- or saline-pairing chambers. In the first drug-pairing trial, we found a significant effect of low-dose (1 mg/kg) amphetamine on locomotor activity by genotype ($F_{2,125} = 7.10$, $P < 0.01$), session ($F_{5,125} = 26.08$, $P < 0.01$) and their interaction ($F_{10,125} = 2.07$, $P < 0.05$). *Post hoc* comparison indicated a significant difference between the WT and *Asic1a*$^{-/-}$ (t = 2.44, $P < 0.05$) and *Asic4*$^{-/-}$ and *Asic1a*$^{-/-}$ (t = 3.74, $P < 0.01$) but not the WT and *Asic4*$^{-/-}$ (t = 1.38, $P = 0.18$). Locomotor activity was greater for *Asic1a*$^{-/-}$ than *Asic4*$^{-/-}$ mice in sessions 1–5 (all $P < 0.01$), and greater for *Asic1a*$^{-/-}$ than the WT only in sessions 2 ($P < 0.01$) and 6 ($P < 0.05$) (Fig. 7A). Locomotor activity was greater in *Asic1a*$^{-/-}$ mice with acute (1 mg/kg) amphetamine treatment. In the saline-pairing trials, we found no significant effect on locomotion of genotype or interaction (data not shown). In the first drug-pairing trial of high-dose (5 mg/kg) amphetamine–CPP the genotype effect was reduced ($F_{2,95} = 2.99$, $P = 0.07$), with a significant effect of session ($F_{5,95} = 14.83$, $P < 0.01$) and interaction ($F_{10,95} = 4.03$, $P < 0.01$). *Post hoc* comparison of the interaction effect indicated a significant difference in sessions 4–6 between *Asic1a*$^{-/-}$ and the WT only ($P < 0.01$) (Fig. 7B). This genotype effect of *Asic1a*$^{-/-}$ in acute amphetamine challenge disagrees with a previous report (Jiang *et al.*, 2013), and possible explanations include different psychostimulants used, genetic background for congenic backcrosses or KO design in generating *Asic1a*$^{-/-}$ mice (Wemmie *et al.*, 2002; Wu *et al.*, 2013). The hyperlocomotion effect increased after repeat amphetamine challenges, a phenomenon called behavioral sensitisation. With low-dose amphetamine–CPP, all three genotypes of mice demonstrated robust behavioral sensitisation with a significant trial effect ($F_{3,73} = 33.85$, $P < 0.01$) but not interaction effect ($F_{6,73} = 0.53$, $P = 0.78$). The genotype effect was significant ($F_{2,73} = 4.47$, $P < 0.05$) and *post hoc* comparison indicated overall higher hyperlocomotion in *Asic1a*$^{-/-}$ than WT and *Asic4*$^{-/-}$ mice (Fig. 7C). With high-dose (5 mg/kg) amphetamine, behavioral sensitisation persisted (significant trial effect: $F_{3,61} = 11.40$, $P < 0.01$, but not interaction effect: $F_{6,61} = 1.76$, $P = 0.12$) in all groups of mice. The genotype effect disappeared ($F_{2,61} = 0.23$, $P = 0.8$), so all three groups demonstrated the same level of locomotion under this condition (Fig. 7D). Without ASIC1a, the hyperlocomotion effect of acute amphetamine may have been potentiated and ASIC4 seemed not involved in this potentiation. Both ASIC1a and ASIC4 had little effect on the phenomena of behavioral sensitisation induced by repeated exposure to a psychostimulant. We used an unbiased procedure to assign the chamber for pairing with drug or saline. In the pretest (habituation) on day 1 of CPP, no groups of mice showed their original preference to these two chambers (Fig. 7E and F). In the final preference test, only *Asic1a*$^{-/-}$ ($t_7 = 4.13$, $P < 0.01$) but not the WT ($t_9 = 1.17$, $P = 0.27$) and *Asic4*$^{-/-}$ ($t_9 = 1.08$, $P = 0.31$) preferred the drug-pairing chamber with low-dose amphetamine (Fig. 7G). This result was consistent with a previous report indicating that mice without ASIC1a showed a stronger preference to the cocaine-paired chamber in CPP (Kreple *et al.*, 2014). All three genotypes showed robust place preference to the drug-pairing

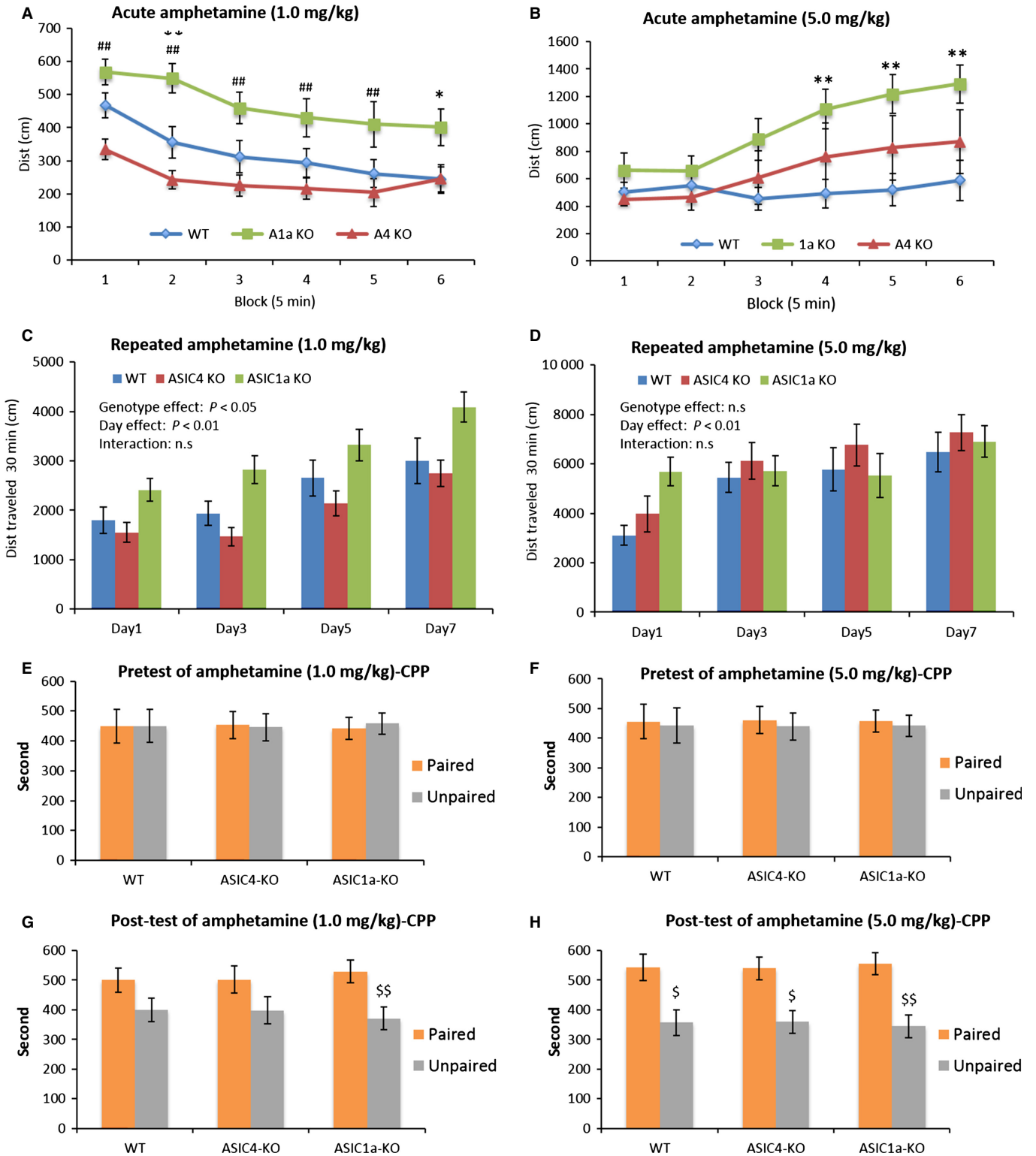

FIG. 7. Amphetamine-induced hyperlocomotion, sensitisation and rewarding effects between *Asic1a*$^{-/-}$ and *Asic4*$^{-/-}$ mice in the CPP task. (A) Acute hyperlocomotion effect after a low-dose (1 mg/kg) amphetamine treatment in the first drug-pairing trial. In contrast to the WT (n = 10) and *Asic4*$^{-/-}$ (n = 10), *Asic1a*$^{-/-}$ mice (n = 8) showed elevated locomotor activity over the 30 min (one session = 5 min). (B) With high-dose (5 mg/kg) acute amphetamine, *Asic1a*$^{-/-}$ (n = 8) mice showed more locomotion than WT (n = 8) but not *Asic4*$^{-/-}$ (n = 6), in sessions 4–6. (C and D) Behavioral sensitisation after repeated amphetamine challenges between genotypes. For each drug-pairing trial, locomotor activity was summed for 30 min and the result indicate that all three groups of mice demonstrated normal progression in locomotion after repeated amphetamine treatment. (E and F) Pretest of chamber preference indicated that under unbiased drug-chamber assignment, no preference was found between the two chambers used for all groups of mice. (G and H) After four drug- and saline-pairing trials, preference for staying in the drug-pairing chamber with (G) low-dose amphetamine and (H) high-dose amphetamine. *P < 0.05, **P < 0.01 compared with WT; $^{\#\#}P$ < 0.01 compared with *Asic4*$^{-/-}$; $^{\$}P$ < 0.05, $^{\$\$}P$ < 0.01 compared with paired chamber.

chamber with high-dose amphetamine (*Asic1a*$^{-/-}$: $t_7 = 2.65$, $P < 0.01$; WT: $t_7 = 2.38$, $P < 0.05$ and *Asic4*$^{-/-}$: $t_7 = 2.39$, $P < 0.05$) (Fig. 7H).

Discussion

Expression of ASIC4 in the CNS

Although ASIC4 was cloned in 2000, its expression and function have not since been investigated (Lin *et al.*, 2015). ASIC4 is a member of the ASIC family, sharing 50–65% sequence identity with other ASIC subtypes and is distributed throughout the CNS. Donier *et al.* (2008) provided the first hint that ASIC4 could counteract the membrane expression and activity of ASIC1a and ASIC3 in a heterologous expressing system. Knockout mice of other ASIC subtypes were generated in the early 2000s, and selective pharmacological tools for ASIC1a (PcTX1, mambalgins) and ASIC3 (APETx2) have been available for many years (Lin *et al.*, 2015). If ASIC4 can interact with other ASIC subtypes to form a heterotrimeric complex and thus modulate the activity of ASIC1a or ASIC3, why this relationship has not been investigated *in vivo* is a mystery. Our genetic mapping result provides a possible explanation: we found that ASIC4 was expressed in only specific cell types in the brain, including CR$^+$ and/or VIP$^+$ interneurons and NG2$^+$ polydendrocytes in the cortex and subcortical structure as well as cerebellar granule cells. Another feature of ASIC4 is its expression in many first-relay nuclei for sensory processing. From the rostral to caudal direction, ASIC4 is positive in the glomerular layer of the olfactory bulb and lateral geniculate nucleus of the thalamus and in the superior colliculus of the midbrain. In the cerebellum, ASIC4 is expressed only in the granule layer; in the spinal cord, ASIC4 is expressed in the central canal and to a lesser extent in the motor neurons and the deep layer of the dorsal horn. Overall, the expression and distribution of ASIC4 in the CNS is much less than that reported for ASIC1a (Price *et al.*, 2014). Using immunostaining techniques, ASIC1a is reported to express in the pyramidal neurons of the cortex and the hippocampus (Alvarez de la Rosa *et al.*, 2003) as well as in the Purkinje cells of the cerebellum and the orexinA-positive neurons in the lateral hypothalamic nucleus (Song *et al.*, 2012). ASIC1a is also expressed in the amygdala, bed nucleus of stria terminalis, habenula, hypothalamus, periaqueductal gray and nucleus accumbens, and is important for modulating the fear response and for rewarding (Coryell *et al.*, 2007, 2008; Kreple *et al.*, 2014). As well, ASIC1a plays important roles in GABAergic interneurons and NG2 cells in the hippocampus (Lin *et al.*, 2010). Together, ASIC4 might be able to interact with ASIC1a in only a small subset of neurons in the brain.

The physiological function of ASIC4

Strong expression of ASIC4 is detected in the pituitary gland and hypothalamus, especially in the paraventricular nucleus, medial preoptic nucleus, arcuate nucleus, lateral hypothalamic nucleus and dorsomedial hypothalamus. These are important nuclei in mammals for regulating feeding, drinking, body-weight regulation and circadian activity (Saper *et al.*, 2005; Meister, 2007). However, ASIC4 mutants show normal body weight, normal proportion of fat to lean tissue and normal free water volume in the body as well as normal home-cage activity under an *ad libitum* feeding schedule. These results exclude an important role for ASIC4 in the pituitary gland and hypothalamus modulating these basic physiological functions (Tables 1 and 2). Also, ASIC4 is not involved in acute thermal and mechanical nociception and motor coordination.

Because ASIC4 can inhibit ASIC1a activity in the heterologous expression system (Donier *et al.*, 2008), we screened possible behavioral phenotypes revealed in the *Asic1a*$^{-/-}$ mice, including (i) impaired fear conditioning task, (ii) severe seizure score after chemoconvulsant treatment, (ii) inability to display appropriate innate fear and less anxiety-like behavior in the OF/EPM task, and (iv) increased addictive potential to psychostimulants. *Asic4*$^{-/-}$ mice and another source of *Asic1a*$^{-/-}$ mice underwent the four behavioral tasks (Wu *et al.*, 2013). Most of the studies describing phenotypes of *Asic1a*$^{-/-}$ mice used the conventional KO line derived from Wemmie's group (Wemmie *et al.*, 2002), but we used the *Asic1a* (exon2–3)-floxed line (Wu *et al.*, 2013). After crossing with the protamine–Cre transgenic mouse, we bred *Asic1a*$^{-/-}$ mice with a deletion of exon2–3 in *Asic1a*. Comparing the phenotype consistency between different KO lines of the same gene is important in behavioral genetics because of different construct designs in the targeted locus and backcrossing to different inbred strains and because they are raised in different environments and under different breeding strategies (Crabbe *et al.*, 1999). Data in contextual fear conditioning almost recaptured the results of previous reports, showing *Asic1a*$^{-/-}$ mutants with the inability to display the proper unconditioned freezing response in the acquisition phase and the conditioned freezing response 24 hr later in the retention phase. However, no difference was found in either phase in *Asic4*$^{-/-}$ mice. The same phenotyping profile was found in the kainic acid-induced seizure test: *Asic1a*$^{-/-}$ but not *Asic4*$^{-/-}$ mutants showed increased lethal rate and Racine score at the low-dose (15 mg/kg) level. Also, *Asic1a*$^{-/-}$ mice demonstrated a 'fearless' phenotype to TMT and 'anxiolytic-like' behavior in the OF and EPM tasks. However, *Asic4*$^{-/-}$ mutants displayed a 'fearful' response to TMT and 'anxiety-like' behavior in the OF and EPM tasks. TMT is a well established animal model for assessing the innate fear response in rodents, and neuronal circuits comprising the olfactory bulb, paraventricular nucleus, periaqueductal gray, bed nucleus of stria terminalis, ventral hippocampus, medial prefrontal cortex and the amygdala are involved in this behavior (Takahashi, 2014). All these nuclei are also involved in generating a proper anxiety response and expressing ASIC4. The contrasting phenotypes between *Asic1a*$^{-/-}$ and *Asic4*$^{-/-}$ mutants in these tasks indicated that these two proteins could interact in the above-mentioned nuclei.

In the amphetamine-induced CPP test, *Asic1a*$^{-/-}$ mice showed an elevated hyperlocomotion effect to both low-dose (1 mg/kg) and high-dose (5 mg/kg) acute amphetamine as compared with *Asic4*$^{-/-}$ mice and the WT. This result is a little different from a previous report claiming that *Asic1a*$^{-/-}$ mutants have less motor-stimulating response to a wide dose range (5, 10, 20 and 30 mg/kg) of cocaine (Jiang *et al.*, 2013). The behavioral sensitisation effect of amphetamine was intact in both *Asic1a*$^{-/-}$ and *Asic4*$^{-/-}$ mice. In the preference test with low-dose amphetamine, only *Asic1a*$^{-/-}$ mice demonstrated robust 'place preference' toward the drug-pairing chamber. This finding is consistent with a recent paper describing *Asic1a*$^{-/-}$ mutants with increased CPP score in the cocaine-pairing chamber (Kreple *et al.*, 2014). The same comparison of the 'preference score' between groups did not show significant differences in our study, which is probably due to the 'unbiased' conditioning procedure we used.

Whether ASIC4 can counteract other ASICs in vivo

In the heterologous expression system, candidate membrane proteins of interest can be co-expressed in the same cells and assayed for their interaction with biochemical and/or electrophysiological methods. A prerequisite of protein–protein interaction that occurs *in vivo*

is that target genes are expressed in the same cell. We have demonstrated that ASIC4 is expressed in three major types of cells in the CNS: CR^+ and/or VIP^+ interneurons, $NG2^+$ polydendrocytes and cerebellar granular cells. These results first exclude the possible interaction of ASIC4 and ASIC3, because ASIC4 is not expressed in adult DRG. CR^+ and/or VIP^+ interneurons are considered the 'disinhibitory circuit motif' and are called interneuron-specific interneurons, that is, these GABAergic interneurons exclusively target other Pv^+- or SOM^+-GABAergic interneurons on their dendritic shafts (Klausberger & Somogyi, 2008). Previous study in the rat hippocampal CA1 and DG identified ASIC1a expression in SOM^+-O-LM cells and Pv^+-fast-spiking basket cells (Weng *et al.*, 2010). From our colocalisation study ASIC4 was absent in these two types of interneurons, and evidence for ASIC1a expression in the CR^+ and/or VIP^+ interneurons is lacking. The possible cells with colocalisation of ASIC1a and ASIC4 are the hippocampal NG2 (Lin *et al.*, 2010) and cerebellar granule cells (Escoubas *et al.*, 2000). Lin *et al.* (2010) demonstrated the expression of ASIC1a in NG2 cells because pharmacological blockage by PcTX1 or genetic KO of ASIC1a eliminated this acid-induced current. Escoubas *et al.* (2000) demonstrated that PcTx1 inhibited the acid-evoked inward current in cerebellar granule cells. Our preliminary data also showed that acid-induced current density was significantly increased in *Asic4*$^{-/-}$ NG2 cells (unpublished data). Thus, the expression of ASIC4 is probably limited to only a small proportion of ASIC1a-positive cells in the CNS, and ASIC4 only counteracts ASIC1a activity in cells involved in the fear and anxiety circuitry. Of note, whilst the *Asic4*$^{-/-}$ phenotypes observed are suggestive of disinhibition of ASIC1a function, until detailed electrophysiological recordings are made this remains a hypothesis.

Summary and future perspective

In this study, we provided a new research direction for understanding ASIC signaling in the brain by mapping ASIC4 expression in an ASIC4-KO/$CreERT^2$-knockin mouse line. Subsequent behavioral phenotyping reconfirms many important *Asic1a*$^{-/-}$ phenotypes and reveals a possible function of ASIC4 in counteracting ASIC1a for modulating the affective state *in vivo*. Unsolved questions about the function of ASIC4 in modulating fear and anxiety include (i) whether ASIC1a is expressed and negatively regulated by ASIC4 in those ASIC4-expressing cells, (ii) in which nuclei in the limbic system ASIC4 downregulate ASIC1a activity and set the proper tone of fear/anxiety, and (iii) how ASIC4 counteracts ASIC1a activity at the molecular level. Protein sequence analysis of ASIC4 suggests two properties distinct from other ASIC subtypes. One is in its N-terminus, an intracellular region rich in Lys residues for ubiquitination. Ubiquitination is important for neurons in controlling the membrane expression of ion channels, and the N-terminus of ASIC4 has been found to interact with polyubiquitin in cultured cells (Donier *et al.*, 2008). Another unique property is in the extracellular loop, where ASIC4 has six N-glycosylation sites as compared with two in ASIC1a. N-glycosylation in the extracellular domain is important for stabilising the expression, trafficking and acid-sensing function of ASIC1a (Jing *et al.*, 2012). Fully glycosylated ASIC4 might stabilise ASIC1a in the heterotrimeric complex and thus enhance the activity of ASIC1a on the membrane.

Conflict of interest

All the authors declare no competing financing interests.

Acknowledgements

The work was supported by Institute of Biomedical Sciences, Academia Sinica and the Drunken Moon Lake Integrated Scientific Research Platform, as well as grants from the Ministry of Science and Technology, Taiwan (MOST103-2325-B-001-015, MOST103-2321-B-001-037). We thank Dr R. M. Liao in the Institute of Psychology, National Cheng-Chi University for technical support and comments in addiction experiments, and the Transgenic Core Facility in the Institute of Molecular Biology, Academia Sinica, Taipei, for producing *Asic4*-KO mice, as well as Ms Chia-Wen Wong for her beautiful artwork in the graphic abstract.

Abbreviations

ASIC, acid-sensing ion channel; CB, calbindin; CPP, conditioned place preference; CR, calretinin; DRG, dorsal root ganglia; EPM, elevated-plus maze; ES, embryonic stem; KO, knockout; NPY, neuropeptide Y; OF, open field; OP, oligodendrocyte progenitor; Pv, parvalbumin; RT, reverse transcription; SOM, somatostatin; TG, trigeminal ganglia; TMT, 2,4,5-trimethylthiazoline; VIP, vasoactive intestinal peptide; WT, wildtype.

References

Abboud, F.M. & Benson, C.J. (2015) ASICs and Cardiovascular Homeostasis. *Neuropharmacology*, doi:10.1016/j.neuropharm.2014.12.012. [Epub ahead of print].

Akopian, A.N., Chen, C.C., Ding, Y., Cesare, P. & Wood, J.N. (2000) A new member of the acid-sensing ion channel family. *NeuroReport*, **11**, 2217–2222.

Alvarez de la Rosa, D., Zhang, P., Shao, D., White, F. & Canessa, C.M. (2002) Functional implications of the localization and activity of acid-sensitive channels in rat peripheral nervous system. *Proc. Natl. Acad. Sci. USA*, **99**, 2326–2331.

Alvarez de la Rosa, D., Krueger, S.R., Kolar, A., Shao, D., Fitzsimonds, R.M. & Canessa, C.M. (2003) Distribution, subcellular localization and ontogeny of ASIC1 in the mammalian central nervous system. *J. Physiol.*, **546**, 77–87.

Ayers, L.W., Asok, A., Heyward, F.D. & Rosen, J.B. (2013) Freezing to the predator odor 2,4,5 dihydro 2,5 trimethylthiazoline (TMT) is disrupted by olfactory bulb removal but not trigeminal deafferentation. *Behav. Brain Res.*, **253**, 54–59.

Baron, A. & Lingueglia, E. (2015) Pharmacology of acid-sensing ion channels - Physiological and therapeutical perspectives. *Neuropharmacology*, doi:10.1016/j.neuropharm.2015.01.005. [Epub ahead of print].

Bartoi, T., Augustinowski, K., Polleichtner, G., Grunder, S. & Ulbrich, M.H. (2014) Acid-sensing ion channel (ASIC) 1a/2a heteromers have a flexible 2:1/1:2 stoichiometry. *Proc. Natl. Acad. Sci. USA*, **111**, 8281–8286.

Cauli, B., Zhou, X., Tricoire, L., Toussay, X. & Staiger, J.F. (2014) Revisiting enigmatic cortical calretinin-expressing interneurons. *Front. Neuroanat.*, **8**, 52.

Chao, H.W., Tsai, L.Y., Lu, Y.L., Lin, P.Y., Huang, W.H., Chou, H.J., Lu, W.H., Lin, H.C., Lee, P.T. & Huang, Y.S. (2013) Deletion of CPEB3 enhances hippocampus-dependent memory via increasing expressions of PSD95 and NMDA receptors. *J. Neurosci.*, **33**, 17008–17022.

Chen, C.C. & Wong, C.W. (2013) Neurosensory mechanotransduction through acid-sensing ion channels. *J. Cell Mol. Med.*, **17**, 337–349.

Coryell, M.W., Ziemann, A.E., Westmoreland, P.J., Haenfler, J.M., Kurjakovic, Z., Zha, X.M., Price, M., Schnizler, M.K. & Wemmie, J.A. (2007) Targeting ASIC1a reduces innate fear and alters neuronal activity in the fear circuit. *Biol. Psychiat.*, **62**, 1140–1148.

Coryell, M.W., Wunsch, A.M., Haenfler, J.M., Allen, J.E., McBride, J.L., Davidson, B.L. & Wemmie, J.A. (2008) Restoring Acid-sensing ion channel-1a in the amygdala of knock-out mice rescues fear memory but not unconditioned fear responses. *J. Neurosci.*, **28**, 13738–13741.

Crabbe, J.C., Wahlsten, D. & Dudek, B.C. (1999) Genetics of mouse behavior: interactions with laboratory environment. *Science*, **284**, 1670–1672.

Dawson, P.A., Steane, S.E. & Markovich, D. (2005) Impaired memory and olfactory performance in NaSi-1 sulphate transporter deficient mice. *Behav. Brain Res.*, **159**, 15–20.

Donier, E., Rugiero, F., Jacob, C. & Wood, J.N. (2008) Regulation of ASIC activity by ASIC4–new insights into ASIC channel function revealed by a yeast two-hybrid assay. *Eur. J. Neuorsci.*, **28**, 74–86.

Du, J., Reznikov, L.R. & Welsh, M.J. (2014) Expression and activity of Acid-sensing ion channels in the mouse anterior pituitary. *PLoS One*, **9**, e115310.

Escoubas, P., De Weille, J.R., Lecoq, A., Diochot, S., Waldmann, R., Champigny, G., Moinier, D., Menez, A. & Lazdunski, M. (2000) Isolation of a tarantula toxin specific for a class of proton-gated Na+ channels. *J. Biol. Chem.*, **275**, 25116–25121.

Feil, R., Wagner, J., Metzger, D. & Chambon, P. (1997) Regulation of Cre recombinase activity by mutated estrogen receptor ligand-binding domains. *Biochem. Bioph. Res. Co.*, **237**, 752–757.

Feldman, D.H., Horiuchi, M., Keachie, K., McCauley, E., Bannerman, P., Itoh, A., Itoh, T. & Pleasure, D. (2008) Characterization of acid-sensing ion channel expression in oligodendrocyte-lineage cells. *Glia*, **56**, 1238–1249.

Galliano, E., Gao, Z., Schonewille, M., Todorov, B., Simons, E., Pop, A.S., D'Angelo, E., van den Maagdenberg, A.M., Hoebeek, F.E. & De Zeeuw, C.I. (2013) Silencing the majority of cerebellar granule cells uncovers their essential role in motor learning and consolidation. *Cell Rep.*, **3**, 1239–1251.

Gregoire, S. & Matricon, J. (2009) Differential involvement of ASIC1a in the basolateral amygdala in fear memory and unconditioned fear responses. *J. Neurosci.*, **29**, 6053–6054.

Grunder, S., Geissler, H.S., Bassler, E.L. & Ruppersberg, J.P. (2000) A new member of acid-sensing ion channels from pituitary gland. *NeuroReport*, **11**, 1607–1611.

Holzer, P. (2015) Acid-sensing ion channels in gastrointestinal function. *Neuropharmacology*, doi: 10.1016/j.neuropharm.2014.12.009. [Epub ahead of print].

Huang, Y., Jiang, N., Li, J., Ji, Y.H., Xiong, Z.G. & Zha, X.M. (2015) Two aspects of ASIC function: synaptic plasticity and neuronal injury. *Neuropharmacology*, doi: 10.1016/j.neuropharm.2014.12.010. [Epub ahead of print].

Jasti, J., Furukawa, H., Gonzales, E.B. & Gouaux, E. (2007) Structure of acid-sensing ion channel 1 at 1.9 A resolution and low pH. *Nature*, **449**, 316–323.

Jiang, Q., Wang, C.M., Fibuch, E.E., Wang, J.Q. & Chu, X.P. (2013) Differential regulation of locomotor activity to acute and chronic cocaine administration by acid-sensing ion channel 1a and 2 in adult mice. *Neuroscience*, **246**, 170–178.

Jing, L., Chu, X.P., Jiang, Y.Q., Collier, D.M., Wang, B., Jiang, Q., Snyder, P.M. & Zha, X.M. (2012) N-glycosylation of acid-sensing ion channel 1a regulates its trafficking and acidosis-induced spine remodeling. *J. Neurosci.*, **32**, 4080–4091.

Klausberger, T. & Somogyi, P. (2008) Neuronal diversity and temporal dynamics: the unity of hippocampal circuit operations. *Science*, **321**, 53–57.

Kreple, C.J., Lu, Y., Taugher, R.J., Schwager-Gutman, A.L., Du, J., Stump, M., Wang, Y., Ghobbeh, A., Fan, R., Cosme, C.V., Sowers, L.P., Welsh, M.J., Radley, J.J., LaLumiere, R.T. & Wemmie, J.A. (2014) Acid-sensing ion channels contribute to synaptic transmission and inhibit cocaine-evoked plasticity. *Nat. Neurosci.*, **17**, 1083–1091.

Krishtal, O. (2015) Receptor for protons: first observations on Acid Sensing Ion Channels. *Neuropharmacology*, doi:10.1016/j.neuropharm.2014.12.014. [Epub ahead of print].

Lin, Y.C., Liu, Y.C., Huang, Y.Y. & Lien, C.C. (2010) High-density expression of Ca2+-permeable ASIC1a channels in NG2 glia of rat hippocampus. *PLoS One*, **5**, e12665.

Lin, S.H., Sun, W.H. & Chen, C.C. (2015) Genetic exploration of the role of acid-sensing ion channels. *Neuropharmacology*, doi:10.1016/j.neuropharm.2014.12.011. [Epub ahead of print].

Macdonald, R., Bingham, S., Bond, B.C., Parsons, A.A. & Philpott, K.L. (2001) Determination of changes in mRNA expression in a rat model of neuropathic pain by Taqman quantitative RT-PCR. *Brain Res. Mol. Brain Res.*, **90**, 48–56.

Meister, B. (2007) Neurotransmitters in key neurons of the hypothalamus that regulate feeding behavior and body weight. *Physiol. Behav.*, **92**, 263–271.

Omerbašić, D., Schuhmacher, L.N., Bernal Sierra, Y.A., Smith, E.S. & Lewin, G.R. (2014) ASICs and mammalian mechanoreceptor function. *Neuropharmacology*, doi: 10.1016/j.neuropharm.2014.12.007. [Epub ahead of print].

Price, M.P., Gong, H., Parsons, M.G., Kundert, J.R., Reznikov, L.R., Bernardinelli, L., Chaloner, K., Buchanan, G.F., Wemmie, J.A., Richerson, G.B., Cassell, M.D. & Welsh, M.J. (2014) Localization and behaviors in null mice suggest that ASIC1 and ASIC2 modulate responses to aversive stimuli. *Genes Brain Behav.*, **13**, 179–194.

Rosen, J.B., Pagani, J.H., Rolla, K.L. & Davis, C. (2008) Analysis of behavioral constraints and the neuroanatomy of fear to the predator odor trimethylthiazoline: a model for animal phobias. *Neurosci. Biobehav. R.*, **32**, 1267–1276.

Saper, C.B., Lu, J., Chou, T.C. & Gooley, J. (2005) The hypothalamic integrator for circadian rhythms. *Trends Neurosci.*, **28**, 152–157.

Sherwood, T.W., Frey, E.N. & Askwith, C.C. (2012) Structure and activity of the acid-sensing ion channels. *Am. J. Physiol.-Cell Ph.*, **303**, C699–C710.

Sluka, K.A. & Gregory, N.S. (2015) The dichotomized role for acid sensing ion channels in musculoskeletal pain and inflammation. *Neuropharmacology*, doi:10.1016/j.neuropharm.2014.12.013. [Epub ahead of print].

Song, N., Zhang, G., Geng, W., Liu, Z., Jin, W., Li, L., Cao, Y., Zhu, D., Yu, J. & Shen, L. (2012) Acid sensing ion channel 1 in lateral hypothalamus contributes to breathing control. *PLoS One*, **7**, e39982.

Takahashi, L.K. (2014) Olfactory systems and neural circuits that modulate predator odor fear. *Front. Behav. Neurosci.*, **8**, 72.

Wemmie, J.A., Chen, J., Askwith, C.C., Hruska-Hageman, A.M., Price, M.P., Nolan, B.C., Yoder, P.G., Lamani, E., Hoshi, T., Freeman, J.H. Jr. & Welsh, M.J. (2002) The acid-activated ion channel ASIC contributes to synaptic plasticity, learning, and memory. *Neuron*, **34**, 463–477.

Wemmie, J.A., Askwith, C.C., Lamani, E., Cassell, M.D., Freeman, J.H. Jr. & Welsh, M.J. (2003) Acid-sensing ion channel 1 is localized in brain regions with high synaptic density and contributes to fear conditioning. *J. Neurosci.*, **23**, 5496–5502.

Weng, J.Y., Lin, Y.C. & Lien, C.C. (2010) Cell type-specific expression of acid-sensing ion channels in hippocampal interneurons. *J. Neurosci.*, **30**, 6548–6558.

Wonders, C.P. & Anderson, S.A. (2006) The origin and specification of cortical interneurons. *Nat. Rev. Neurosci.*, **7**, 687–696.

Wu, W.L., Lin, Y.W., Min, M.Y. & Chen, C.C. (2010) Mice lacking Asic3 show reduced anxiety-like behavior on the elevated plus maze and reduced aggression. *Genes Brain Behav.*, **9**, 603–614.

Wu, W.L., Cheng, C.F., Sun, W.H., Wong, C.W. & Chen, C.C. (2012) Targeting ASIC3 for pain, anxiety, and insulin resistance. *Pharmacol. Therapeut.*, **134**, 127–138.

Wu, P.Y., Huang, Y.Y., Chen, C.C., Hsu, T.T., Lin, Y.C., Weng, J.Y., Chien, T.C., Cheng, I.H. & Lien, C.C. (2013) Acid-sensing ion channel-1a is not required for normal hippocampal LTP and spatial memory. *J. Neurosci.*, **33**, 1828–1832.

Xu, X., Roby, K.D. & Callaway, E.M. (2010) Immunochemical characterization of inhibitory mouse cortical neurons: three chemically distinct classes of inhibitory cells. *J. Comp. Neurol.*, **518**, 389–404.

Zeng, W.Z., Liu, D.S., Duan, B., Song, X.L., Wang, X., Wei, D., Jiang, W., Zhu, M.X., Li, Y. & Xu, T.L. (2013) Molecular mechanism of constitutive endocytosis of Acid-sensing ion channel 1a and its protective function in acidosis-induced neuronal death. *J. Neurosci.*, **33**, 7066–7078.

Ziemann, A.E., Schnizler, M.K., Albert, G.W., Severson, M.A., Howard, M.A. 3rd, Welsh, M.J. & Wemmie, J.A. (2008) Seizure termination by acidosis depends on ASIC1a. *Nat. Neurosci.*, **11**, 816–822.

Ziemann, A.E., Allen, J.E., Dahdaleh, N.S., Drebot, I.I., Coryell, M.W., Wunsch, A.M., Lynch, C.M., Faraci, F.M., Howard, M.A. 3rd, Welsh, M.J. & Wemmie, J.A. (2009) The amygdala is a chemosensor that detects carbon dioxide and acidosis to elicit fear behavior. *Cell*, **139**, 1012–1021.